The Topology of Molecules with Twelve Fused Phenyl Rings ([12]Circulenes): Rings, Infinitenes, and Möbius Infinitenes

Steven M. Bachrach

Artis College of Science and Technology, Radford University, Radford VA 24142 USA

sbachrach@radford.edu

Abstract

Following the recent preparation of infinitene (*J. Am. Chem. Soc.* **2022**, *144*, 862-871), a computational (ωB97XD/6-311G(d)) exploration of 42 isomeric compounds with 12 fused phenyl rings identified structures with linking number of zero (ring, saddle, and ribbon shapes), two (infinitene-like shape), and one (Möbius infinitene shape) is reported. An infinitene isomer composed of two [5]helicene fragments connected to two stacked phenyl rings and a Möbius infinitene isomer are identified that are more stable than the known infinitene. The energies of the structures are examined by assessing their strain energies, π-stacking, and possible aromaticity. Examples of fused phenyl molecules with linking numbers of 3, 4, 5, and 6 are shown, indicating the potential topological range that these molecules can possess.

Introduction

With the recent synthesis, isolation, and characterization of large molecules composed of fused aromatic rings, exemplified by graphene sheets, nanorods, and fullerenes, chemists and physicists were inspired to create and examine smaller fragment molecules.[1] These have included planar and curved graphenes,[2] buckybowls,[3] and nanobelts.[4] Interest has expanded beyond fused systems to include molecules like the cycloparaphenylenes,[5] where the aromatic rings are linked but not fused. All of these novel small polycyclic aromatic molecules may provide interesting optical and electrical properties,[6] especially as semiconductors.

Members of the family of molecules composed of 12 fused phenyl rings have garnered interest for decades. Kekulene **1** (Figure 1) was first prepared by Diederich in 1978.[7] Its aromaticity has been much discussed, and a recent atomic force microscopy study suggests that **1** consists of alternating benzene and non-aromatic rings.[8] Itami synthesized the nanobelt **2**.[4a] It is a cyclophenacene where the rings alternate in an ortho and a para fusion pattern. The analogue with the all ortho-fusion is [12]-circulene **3**. Quantum computations indicates that **3** has a saddle geometry.[9] The cycloacene **4** has the twelve rings fused in a para fashion. This molecule, like **3**, has not yet been prepared, though this family of molecules was proposed as far back as 1954.[10] These four molecules have very different geometries: planar (**1**), ribbon (**2** and **4**) and saddle (**3**).

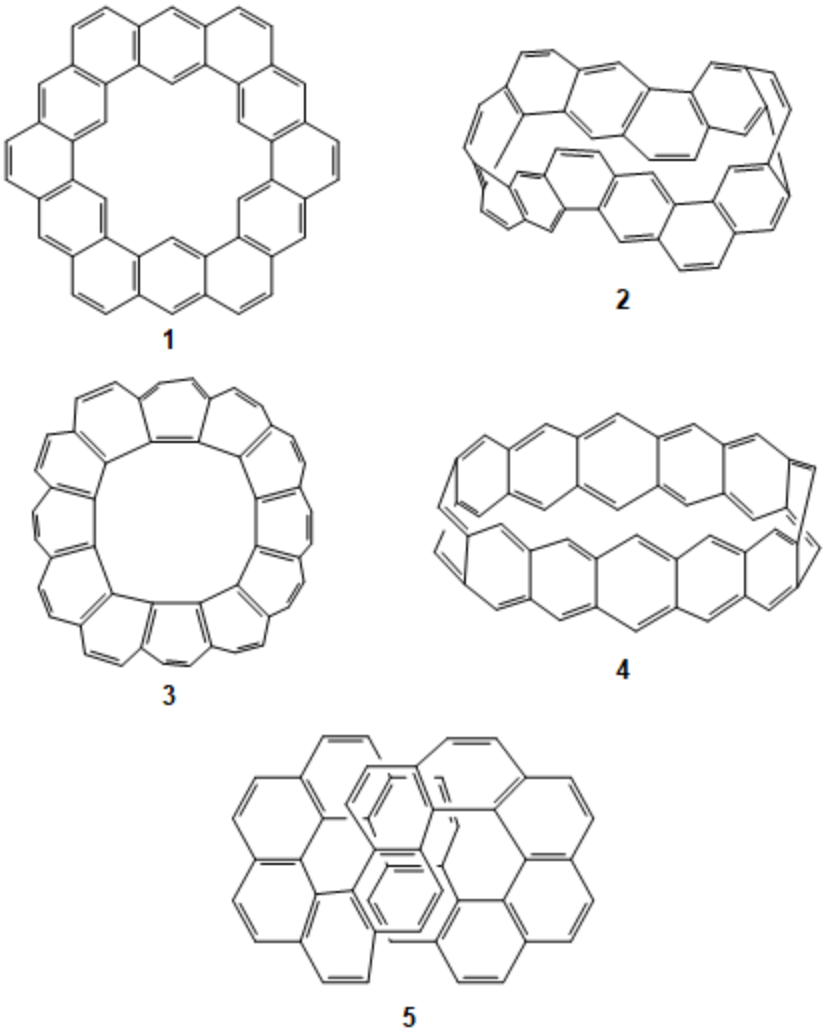

Figure 1. Structures of some [12]circulenes.

In 2021, Itami reported the synthesis of infinitene **5**, consisting of twelve fused phenyl rings that form a figure eight, or an infinity symbol.[11] This molecule is topologically distinct from **1**-**4**. These four molecules have linking number[12] L_k of zero, indicating a molecule whose graph can be written within a plane. The linking number of infinitene **5** is two, indicating that the molecule makes one full twist. It can be thought of as a ribbon that is cut, one end twisted one full rotation, and then stitched back together. The graph of **5** cannot be drawn in a plane without some edges crossing over each other.

The synthesis of **5** inspired our pursuit of a Möbius form of twelve fused phenyl rings. Many studies have explored a variety of aromatic molecules with a Möbius topology, including polyenes, porphyrins, and cycloparaphenylenes.[13] The key distinction of the Möbius topology is its half twist: a ribbon is cut, one end is twisted one-half rotation, and then the ends of the ribbon are stitched together. A Möbius system has linking number of one. More generally, the linking number of Möbius systems is odd while Hückel systems have L_k values that are even. The molecular graphs of Möbius systems cannot be drawn in a plane without edges that cross.

For simplicity, we adopt the term *circulene* to describe any poly-fused-phenyl system irrespective of whether the fusion is ortho or para. It allows for a molecule to contain a mix of these connections. This terminology allows for **1-5** to all be incorporated into the category of [12]circulene.

This article reports a DFT computational survey of a variety of [12]circulenes that demonstrate a range of topologies. This category spans linking numbers of 0, 1, and 2, with shapes that range from planar, to ribbon, to saddle, to half-twisted to full-twisted. Examples of some even more twisted circulenes conclude this report.

Computational Methods

The structures of all compounds were fully optimized, with symmetry imposed where possible, at ωB97XD/6-311G(d).[14] Analytical frequencies were computed to confirm that every structure is a local energy minimum. The unscaled zero-point vibrational frequencies were used to compute enthalpies at 298 K. NMR chemical shifts were computed at B3LYP/6-31+G(d,p) with solvent (chloroform) modeled using SMD and the ωB97XD/6-311G(d) optimized geometries. All computations were performed using *Gaussian-16*.[15] Linking numbers were computed using the *LinkTW* and *LinkTWM* programs.[16]

Results and Discussion

Designating [12]circulene configuration

In order to aid in differentiating the many different [12]circulenes, we propose the following nomenclature scheme. The circulenes will be considered as composed of a series of three fused-phenyl rings. A symbol will be applied to each ring of the circulene based on its type, such that every unique [12]circulene will have a unique 12-character designation.

There are two molecules composed of three fused phenyl rings: anthracene and phenanthrene. The ring in the central position of an anthracene unit will be designated by "A" (Figure 2). There are two orientations for phenanthrene. If moving left to right through the centers of the three rings is clockwise, that central ring will be designated "C", while the counterclockwise connection will be designated "D" (Figure 2).

Application of this rule to two simple [5]acenes **6** and **7** is shown in Figure 2. The designation for the three central rings is DAD for **6** and DAC for **7** when viewing left to right. When viewing right to left, the designation for **7** is unchanged, but is CAC for **6**. Furthermore, if the orientations of the two molecules is flipped, as in the bottom of Figure 2, the designations for **6** are unchanged, but for **7** it is CAD. The multiple designations for each molecule is a result of the combinatorics: the arbitrary orientation of the molecule should not matter. We opt to choose the designation that has more C rings and has them earlier in the designation.

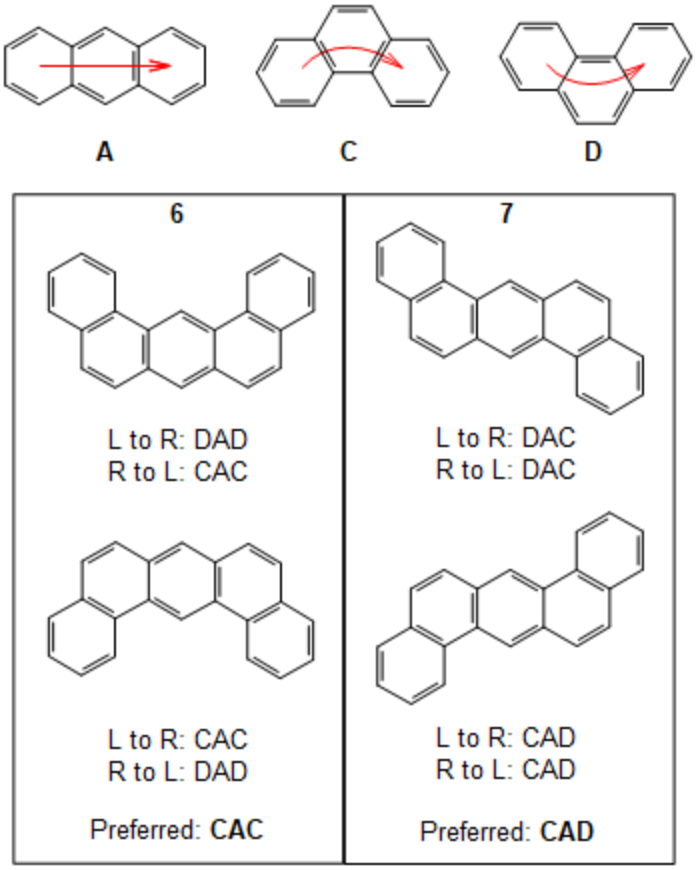

Figure 2. Definition of A, B, and C connectivity, with application to **6** and **7**.

Combinatorial equivalencies are prevalent in the [12]circulenes. The starting ring position is arbitrary, and so for any random [12]circulenes, one could start at any of the rings and then proceed arbitrarily clockwise or counterclockwise about the macrocycle. This leads to 24 different designations for the same molecule. This is a well-known problem, often contextualized as asking for the number of unique necklaces formed of 12 beads, where each bead can be of one of three colors.[17] The redundancies here reduce the number of unique configurations from 3^{12}=531,441 to 44,368. Symmetry considerations further reduce the number of unique configurations, but this number remains above 20,000.

The designations of **1-5** are listed in Table 1. Examination of all possible [12]circulenes is a daunting prospect, and so a small representative survey of [12]circulenes is reported here, demonstrating the topological range of this family. Since these [12]circulenes are very similar in structure, the InChIs and InChIKeys[18] of all reported compounds were also determined and helped to confirm that each compound is unique. These InChIs and InChIKeys are given in the Supporting Materials.

Table 1. Nomenclature of **1-5**.

Compound	designation
1	CACACACACACA
2	CADACADACADA
3	CCCCCCCCCCCC
4	AAAAAAAAAAAA
5	CCCCCCDDDDDD

Strain energy

Simple examination of the 2-D graphs of circulenes **1-5** suggest that many of these molecules will exhibit significant strain, along with various degrees of aromaticity. Disentangling these two countervailing effects is impossible since one cannot choose a reference system that uniquely accounts for strain without also affecting the aromaticity; closure of reference compound to the macrocyle simultaneously affects both aromaticity and strain.[19]

The group equivalent reaction[20] preserves chemical groups, is homodesmotic,[21] and attempts to conserve significant bond relationships. The group equivalent reaction to assess the strain energy of **5** is shown as Reaction 1. This reaction conserves the number of ortho acene fusions, as opposed to Reaction 2 employed by Itami.[11] The energy estimated by these two reactions is quite different: 55.1 kcal mol^{-1} using Reaction 1 and 42.2 kcal mol^{-1} with Reaction 2. This 13 kcal mol^{-1} difference is solely

attributable to inconsistencies in the *reference compounds* and has nothing to do with the strain of the macrocyle itself. Reaction 1, which conserves more structural features of the macrocyle than does Reaction 2, provides the better metric.

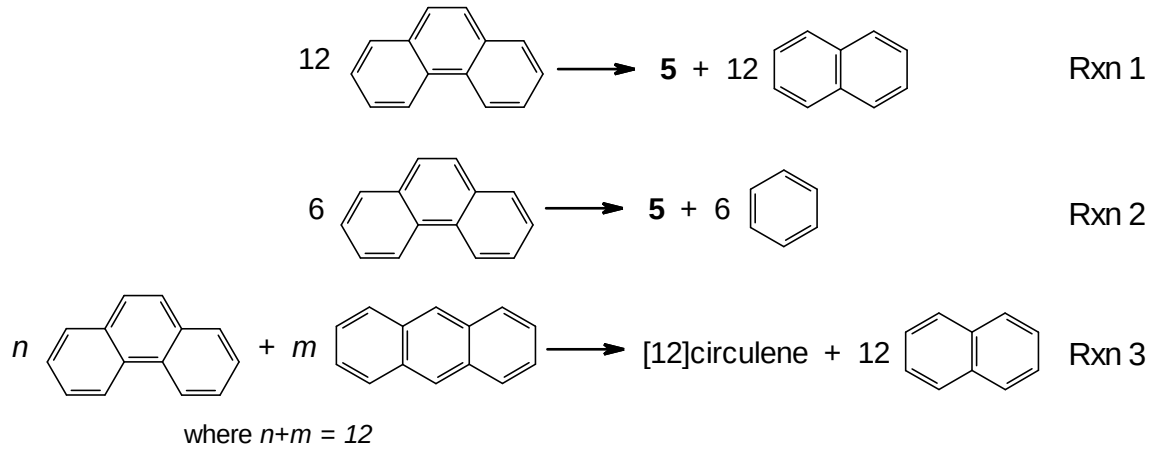

Reaction 1 can be generalized for any [12]circulene by Reaction 3. Reaction 3 conserves the number of anthracenyl and phenanthrenyl (combining both types C and D) subunits. It is important to keep in mind that comparisons of energies provided by Reaction 3 reflect a combination of differences in strain energies *and* differences in aromatic stabilizations, though for simplicity we refer to them as simply *strain energies*.

[12]Circulenes with linking number of zero: rings

The first set of [12]circulene isomers all have linking number of zero. These are molecules with a ring geometry. They fall into three broad generic groupings. Molecules in the first group have a roughly planar structure. The second group has a saddle-like geometry. The last group has a ribbon-like geometry. A total of 19 different [12]circulenes with a ring geometry have been computed, shown in Figure 3.

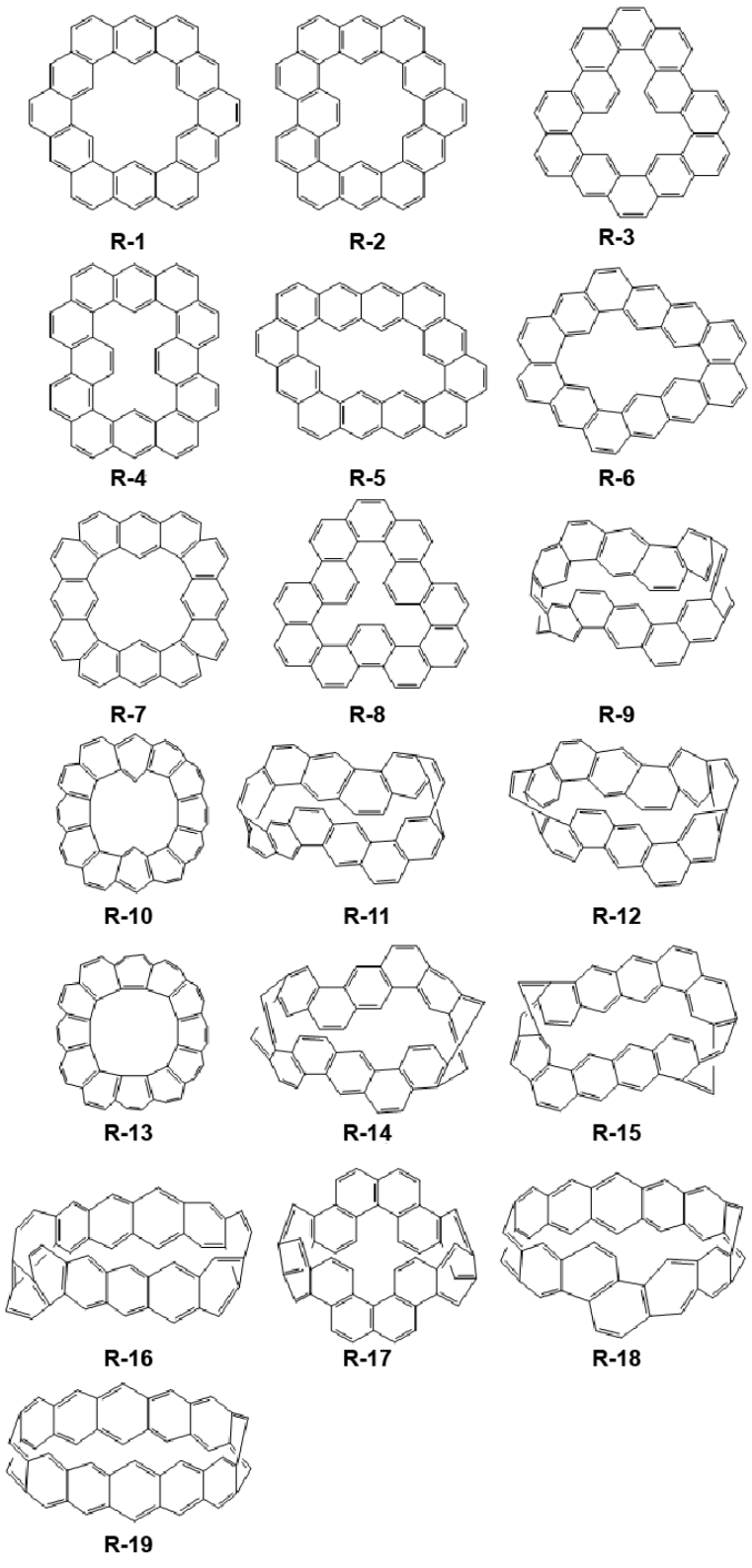

Figure 3. [12]circulene ring isomers

The most stable [12]circulene isomers have planar-like structures. The most stable isomer overall is **R-1**, known as kekulene. It is nearly 8 kcal mol^{-1} more stable than the next lowest energy member **R-2**. **R-1** has been controversially called "superaromatic".[8, 22] It is the only example of a [12]circulene whose strain energy is negative; it is *more stable* that the reference of six anthracene molecules and six phenanthrene molecules by 16 kcal mol^{-1} (Table 2). While the term "superaromatic" has been discounted, **R-1** certainly expresses an unusual stability. The extensive π-delocalization about this perfectly planar molecule (see Figure 4) is unique to this class of [12]circulenes. Any change to the alternating "CAC" pattern results in a non-planar structure that must have less than ideal π-overlaps, and a higher relative energy.

Table 2. Relative energy and strain energy (kcal mol^{-1}) of the ring [12]circulenes (**R-1** – **R-19**)

Cmpd	Designation	E_{rel}	SE
R-1	CACACACACACA	0.00	-16.08
R-2	CACACACACCDC	7.79	4.41
R-3	CACACCDCCCDC	15.03	24.36
R-4a	CACCDCCACCDC	18.27	27.59
R-4b	CACCDCCACCDC	18.36	27.68
R-5	CAACACCAACAC	30.02	13.94
R-6	CCACAACCAACA	35.27	19.19
R-7	CCACCACCACCA	45.83	42.45
R-8	CCCDCCCDCCCD	57.20	79.23
R-9	CDACDADCADCA	104.02	100.64
R-10	CCCCCACCCCCA	104.16	113.48
R-11	CADACADACADA	104.81	88.73
R-12	CCCDACDCDCAD	107.80	117.13
R-13	CCCCCCCCCCCC	107.89	129.91
R-14	CADCAACADAAD	112.09	96.01
R-15	CAACAADAADAA	117.13	88.35
R-16	CAAAACDCAAAA	126.07	97.29
R-17	CCDDCCDDCCDD	130.52	152.54
R-18	CDAAAAAAAAAA	190.98	149.50
R-19	AAAAAAAAAAAA	213.93	159.75

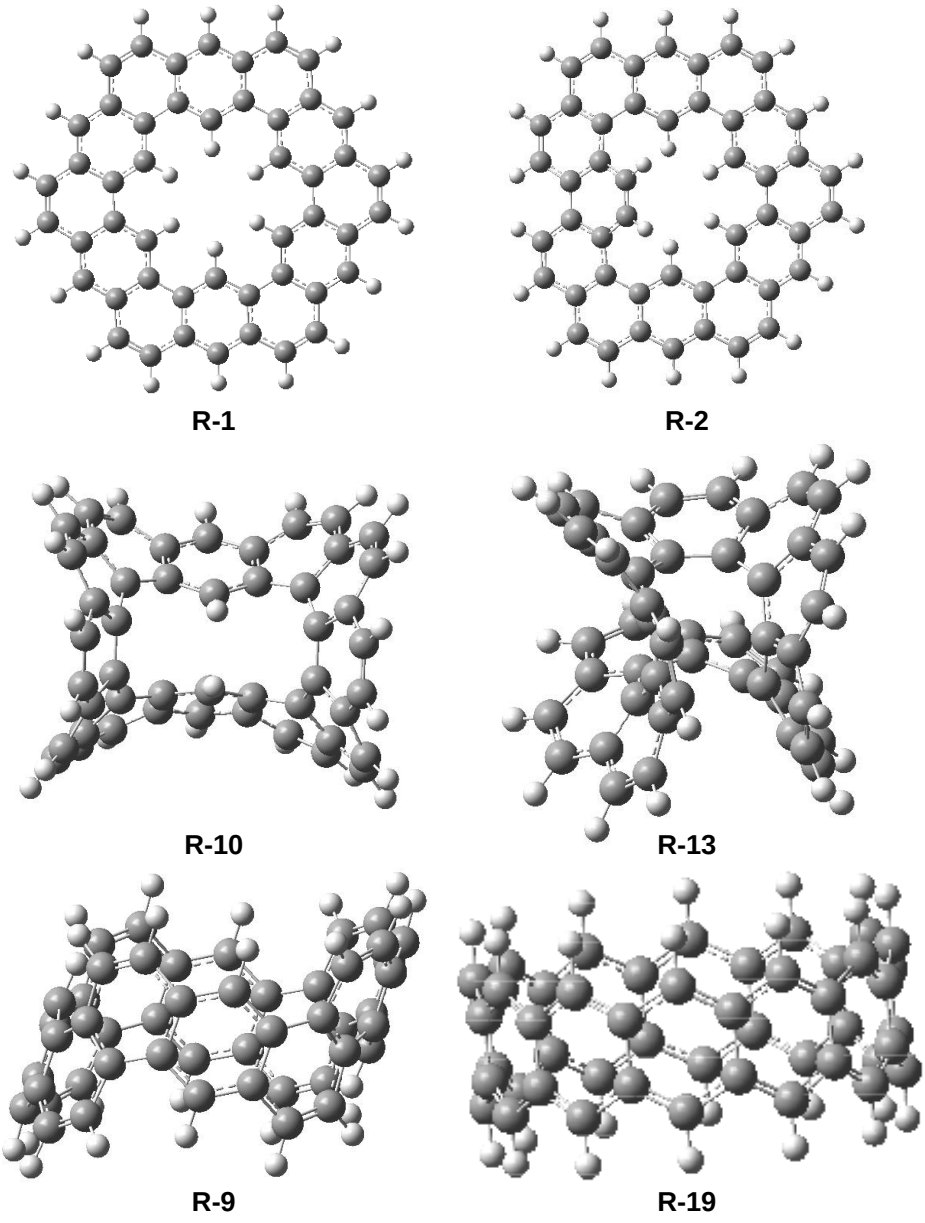

Figure 4. Structures of representative ring-like [12]circulene isomers

The next three lowest energy [12]circulene isomers (Table 2) exchange some "A" connections with "C" or "D" connections. This results in a having at least two regions of four rings fused in a helicene arrangement that must adopt a non-planar arrangement to avoid hydrogen clashes. **R-2** has two such helicene regions (Figure 4); it is non-planar and is about 8 kcal mol^{-1} higher in energy than **R-1**. **R-3** has a five-ring helicene and two four-ring helicene regions and is 15 kcal mol^{-1} less stable than **R-1**. **R-4** has

four helicene regions and its two conformations (of C_{2v} or C_{2h} symmetry) both are about 18 kcal mol^{-1} higher in energy than **R-1**.

The helicene regions and the overall non-planar structure manifest in increased strain energy. **R-2** has a strain energy of 4 kcal mol^{-1}, while **R-3** and **R-4** are strained by more than 24 kcal mol^{-1}. While the rough trend is for increasing RSE to track with increasing relative energy of the isomers, it is not a linear relationship. For example, while **R-2** is 7.8 kcal mol^{-1} higher in energy than **R-1**, its RSE is 20 kcal mol^{-1} more than that of **R-1**. This can be attributed to differences in the number of anthracenes and phenanthrenes as the reference. Phenanthrene is lower in energy than anthracene, and so a circulene with more "C" and "D" connections will have a lower reference energy. **R-2** has two more "C/D" connections than does **R-1**, and all things being equal, it should be more stable than **R-1**. In fact, **R-2** is less stable than **R-1** so it must be more strained.

The second set of [12]circulenes with *Lk*=0 have a saddle structure. The saddle geometry is favored by isomers that have a preponderance of "C" connections. The computational study by Hopf[9] of circulenes with only "C" connections indicated a saddle geometry when the compound had seven or more fused rings. **R-13** is this example for the [12]circulenes, made up of 12 "C" connections (Figure 4). It is much higher in energy than **R-1** (108 kcal mol^{-1}) with a RSE of nearly 130 kcal mol^{-1}. Replacing two "C" connections with "A" connections (**R-10**) maintains the saddle geometry, and while it does reduce both the relative and strain energies, it remains quite high in energy.

The last set of ring circulenes represent ribbon geometries. In general, these ribbon isomers are among the highest energy [12]circulenes. The lowest energy isomer is **R-9**, lying 104 kcal mol^{-1} above **R-1**. The isomer **R-11** has been prepared, again by the Itami group, though our estimate of its strain energy, 89 kcal mol^{-1}, is substantially lower than their estimate of 120 kcal mol^{-1}.[4a] The ribbon isomer having all "A" connections **R-19** is the highest energy [12]circulene: it is 213 kcal mol^{-1} higher in energy than **R-1**. It is also the most strained isomer, with an RSE of 160 kcal mol^{-1}. Every phenyl ring must be

significantly distorted from planarity in order to close the ribbon. Linear acene fragments of **R-19** were compared to their planar analogues to estimate this non-planar distortion. Extrapolating the energy difference to linear [12]acene suggests a strain energy of about 135 kcal mol^{-1} simply due to distortion from non-planarity (see Supporting Materials for details).

[12]Circulenes with linking number of two: infinitenes

The first [12]circulene with a linking number of two was prepared by the Itami group and reported in 2022.[11] **I-2** (referred to in the Introduction as **5**) was named *infinitene* for its structural resemblance to the infinity symbol. The Itami group employed Reaction 2 and PBE0/6-311+G(d,p) energies to estimate the strain energy of **I-2** at 60.2 kcal mol^{-1} (see Table 3). Reaction 2 underestimates the strain energy principally by using benzene as a reference compound. Reaction 1 conserves the number of bridgehead and non-bridgehead aromatic carbon atoms, along with the number of phenanthrenyl units (and anthracenyl units with Reaction 3). The strain energy is about 13 kcal mol^{-1} larger with Reaction 1 than with Reaction 2.

The figure-eight (or infinity sign) structure of **I-2** enables a π-stacking arrangement at the crossover region. The distance between the center of the stacked phenyl rings in the experimental structure of **I-2** is 3.152−3.192 Å. Itami and coworkers selected the PBE0/6-311+G(d,p) method in part for its prediction of this distance of 3.192 Å, which is at the outer edge of the experimental range. Grimme[23] has noted that π-stacking compounds require a density functional that accounts for dispersion, something that PBE0 lacks. Both B3LYP/6-311G(d) and ωB97X/6-311G(d) predict (Table 3) long π-stacking distances that are dramatically reduced when a dispersion correction is included. Both of these corrected methods predict a shorter stacking distance, and the distance in the ωB97XD/6-311G(d) optimized structure is 3.163 Å, close to the low end of the experimental range.

Computation of the strain energies of **R-1**, **R-7**, and **R-9** at B3LYP/6-311G(d), B3LYP-D3/6-311G(d), ωB97X/6-311G(d), and ωB97XD/6-311G(d) (See Table 3) shows a difference of less than 4 kcal

mol^{-1} with and without the dispersion correction. This is opposed the large difference (15-17 kcal mol^{-1}) with the inclusion of a dispersion correction for **I-2**. The ring structures have no π-stacking and thus only a small effect is seen with the dispersion correction. When a molecule (like **I-2**) possesses π-stacking, the dispersion correction is necessary. Thus, the structural and strain energy arguments supports the selection of the ωB97XD/6-311G(d) method for this study of the [12]acenes. So, the best estimate of the strain energy of **I-2**, using Reaction 1 and ωB97XD/6-311G(d) energies, is 55.1 kcal mol^{-1}.

Table 5. Strain energy (kcal mol^{-1}) and π-stacking distance (Å) of **I-2** computed with various methods.

Method	SE (Rxn 1)	SE (Rxn 2)	*r*(π-stack)
ωB97X/6-311G(d)	72.0	58.4	3.198
ωB97X-D/6-311G(d)	55.1	42.2	3.163
PBE0/6-311G(d)	76.0	65.7	3.138
PBE0/6-311+G(d,p)[11]		60.2	3.192
B3LYP/6-311G(d)	74.7	68.8	3.248
B3LYP-D3/6-311G(d)	49.3	39.8	3.134
Expt[11]			3.152−3.192

Eight different configurations of [12]circulene (see Figure 5) were identified that have an infinitene-like structure, i.e. the figure-eight arrangement with a linking number of 2. Their geometries are shown in Figure 6, and their relative energies are listed in Table 4. All of these infinitenes possess a set of 4-6 consecutive "C" connections (with **I-8** having a "CCACC" stretch) and a set of 4-6 consecutive "D" connections (again with **I-8** having a "DDADD" stretch). These two regions create the turns of their figure-eight structures.

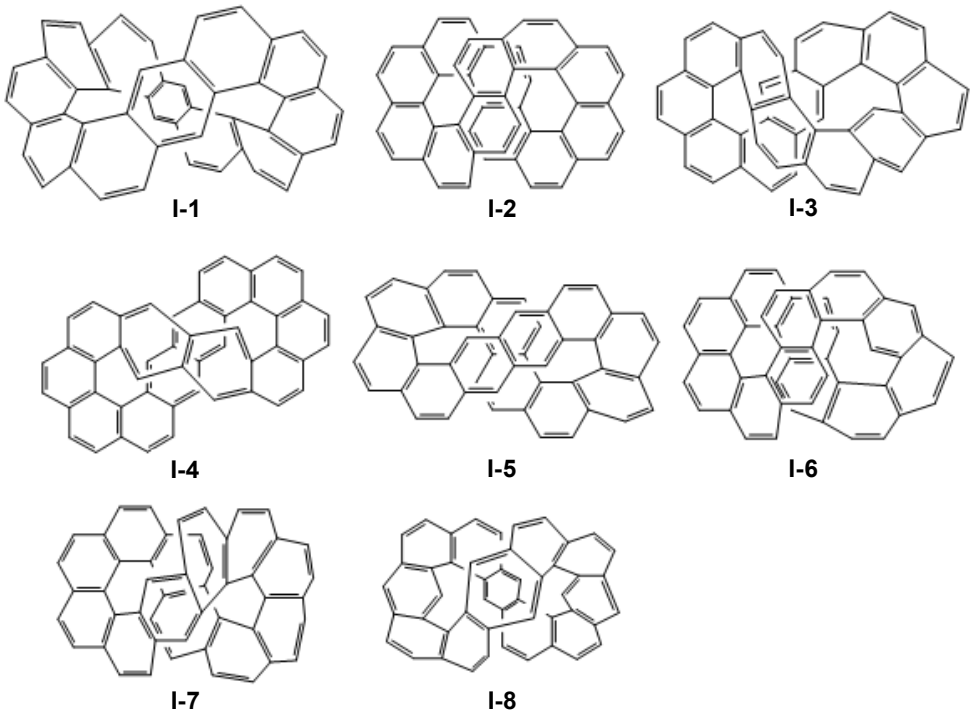

Figure 5. [12]circulene infinitene isomers

Table 4. Relative energy and strain energy (kcal mol^{-1}) of the infinitene-like [12]circulenes (**I-1** – **I-8**)

Cmpd	Designation	E_{rel}[a]	SE
I-1	CCCCCADDDDDA	32.09	41.41
I-2	CCCCCCDDDDDD	33.11	55.13
I-3	CCCCCADDDADD	38.30	47.62
I-4	CCCCAADDDDAA	38.80	35.42
I-5	CCCCCDDDDDAA	45.33	54.65
I-6	CCCCCDDADDDD	54.14	69.81
I-7	CCCCCCADDDDD	60.45	76.12
I-8	CCACCADDADDA	94.01	90.64

[a]Energy relative to that of **R-1**.

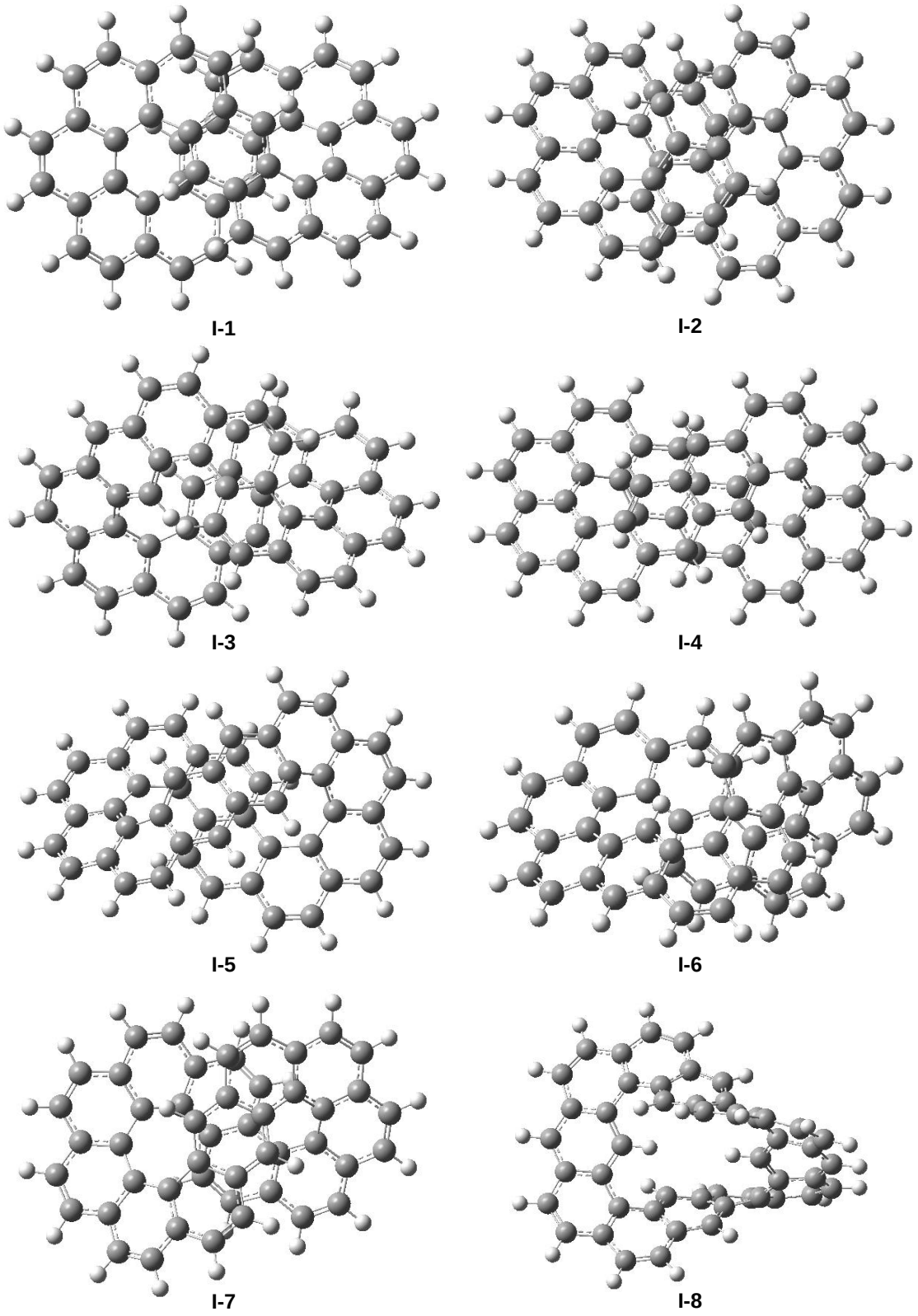

Figure 6. Structures of [12]circulene infinitene isomers

Interestingly, the infinitene that the Itami group prepared (**I-2**) is not the lowest energy infinitene isomer. Rather, **I-1** lies 1 kcal mol^{-1} below **I-2**. It is also significantly less strained than **I-2**: 41.4 kcal *vs*. 55.1 kcal mol^{-1}. **I-1** is characterized by two stacked phenyl rings at the crossing point of the figure eight. These two phenyl rings are the central ring of an anthracenyl fragment ("A" type configuration). The loops are closed by five consecutive "C"-type phenyl rings on one side and five consecutive "D" types on the other side. The structural features are in contrast to those of **I-2**, namely, two stacked naphthalenyl groups in the crossing region, part of six consecutive "C"-type and six consecutive "D" type phenyl rings.

The distance between the centers of the two stacked anthracenyl fragments in **I-1** is 3.061 Å. As discussed with **I-2**, this distance increases to 3.081 Å when the dispersion correction is removed. More important than that structural effect is that the strain energy of **I-1** is about 14 kcal mol^{-1} larger at ωB97X/6-311G(d) than when the dispersion correction is included.

Another interesting infinitene is **I-4**, characterized by having two stacked naphthalenyl groups, each part of crossing tetracenyl moieties. While **I-4** is 6.7 kcal mol^{-1} less stable than **I-1**, it has the lowest strain energy of the eight computed infinitenes, only 35.4 kcal mol^{-1}.

The strain energies of **I-1**, **I-2**, and **I-4** were furthered analyzed by assessing one source of strain, due to the distortion of the helicene component, and a source of stabilization, π-stacking. For **I-2** and **1-4**, the energy of the hexahelicene fragment fixed to its geometry in the infinitene is compared to the energy of fully optimized hexahelicene. For **1-1**, the same energy comparison was made for the pentahelicene fragment. (More details can be found in the Supporting Information.) The helicene distortion energies are listed in Table 5. The two helicene components in **I-4** are each 7 or 12 kcal mol^{-1} less strained than those in **I-1** or **I-2**, respectively.

Table 5. Helicene distortion energy and π-stacking energy in **I-1**, **I-2**, and **I-4**.[a]

	Helicene distortion	π-stacking
I-1[b]	42.8	-9.6
I-2[c]	53.4	+3.5
I-4[c]	29.4	-8.4

[a]See Supporting Information for further details. [b]Helicene with five phenyl rings and anthracene dimer. [c]Helicene with six phenyl rings and naphthalene dimer.

To assess the π-stacking energy, the dimers of naphthalene (for the crossing in **I-2** and **I-4**) and anthracene (for the crossing in **I-1**) were fully optimized. The two molecules were then separated to the π-stacking distance found in the respective infinitenes, and a rotational potential energy surface was computed. Using this PES, the dimer energy was estimated based on the rotational angle in each infinitene. (Again, more details can be found in the Supporting Information.) The estimated π-stacking energies are listed in Table 5. The π-stacking is stabilizing by about 9 kcal mol^{-1} for both **I-1** and **I-4**, but destabilizing (i.e. less stable than two isolated naphthalene molecules) by 3.5 kcal mol^{-1} for **I-2**.

From Table 4, the strain energy these three infinitenes are ordered: **I-4** < **I-1** < **1-2**. The components of the strain energy listed in Table 5 mimic these strain energies nicely. **I-4**, the least strained infinitene, has the lowest helicene distortion energy and significant π-stacking stabilization. **I-1**, experiences slightly more π-stacking stabilization, offset by more helicene distortion than **I-4**. The most strained of these thee infinitenes, **I-2**, has the greatest helicene distortion energy and its π-stacking is destabilizing.

The upshot is that in addition to the already prepared infinitene **I-2**, a number of other infinitene isomers should be viable synthetic targets.

[12]Circulenes with linking number of one: Möbius infinitenes

The last set of [12]circulenes that were explored are those that have a Möbius topology. Möbius infinitenes will have linking number of one, indicating that a half-twist occurs as one traverses across the face of the molecule, coming out on the opposite face. A second traverse returns to the original starting point. A total of fifteen different configurations of [12]circulene were identified that have a Möbius topology, **M-1** through **M-15**, see Figure 7. The structures of the eight lowest energy Möbius infinitenes are displayed in Figure 8. The relative energies and strain energies of the Möbius infinitenes are listed in Table 6. For all but two of these Möbius infinitenes, the connections of the rings are of the C-type, with a small number of "A" connections providing the means for the half-twist.

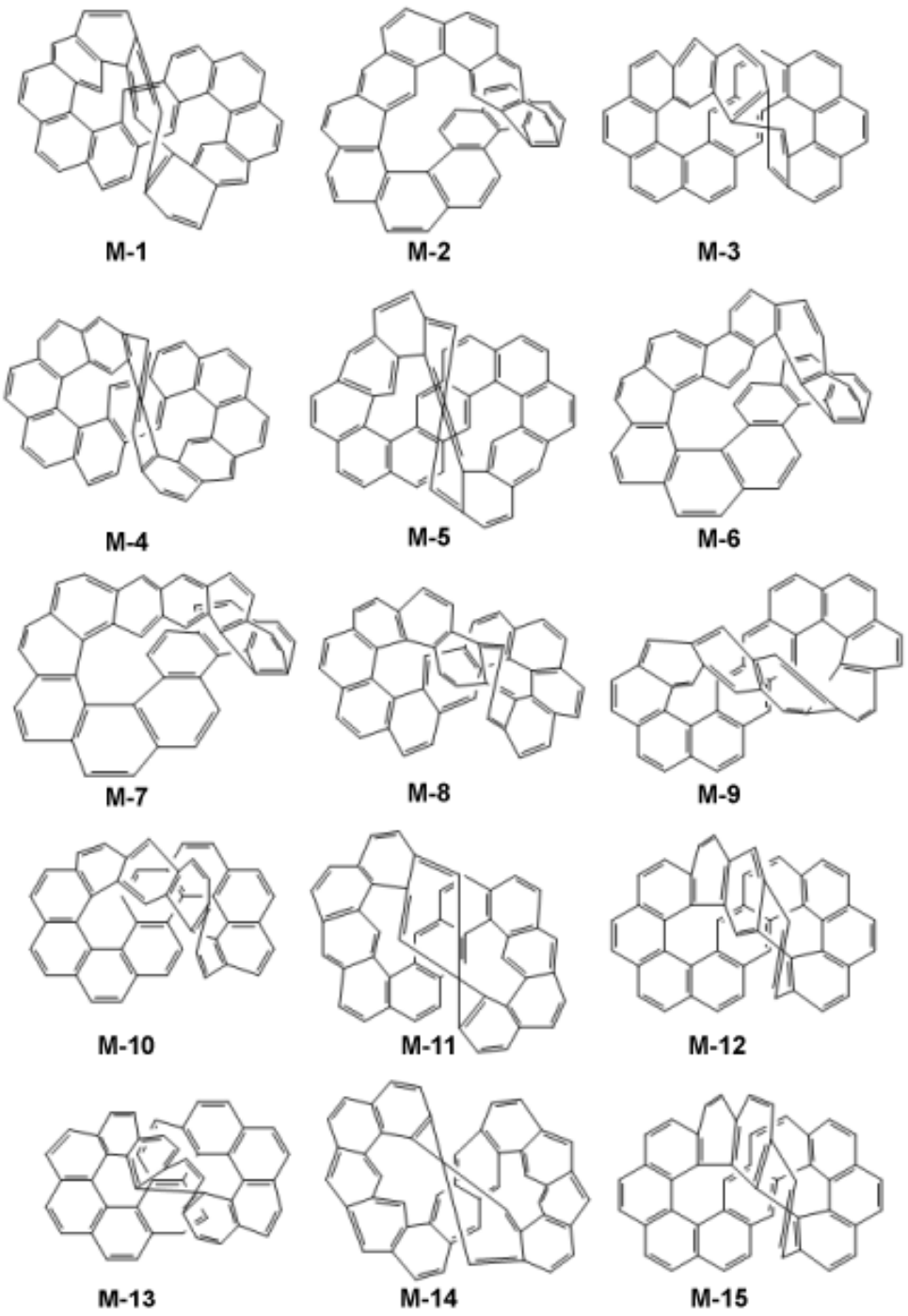

Figure 7. [12]circulene Möbius infinitene isomers

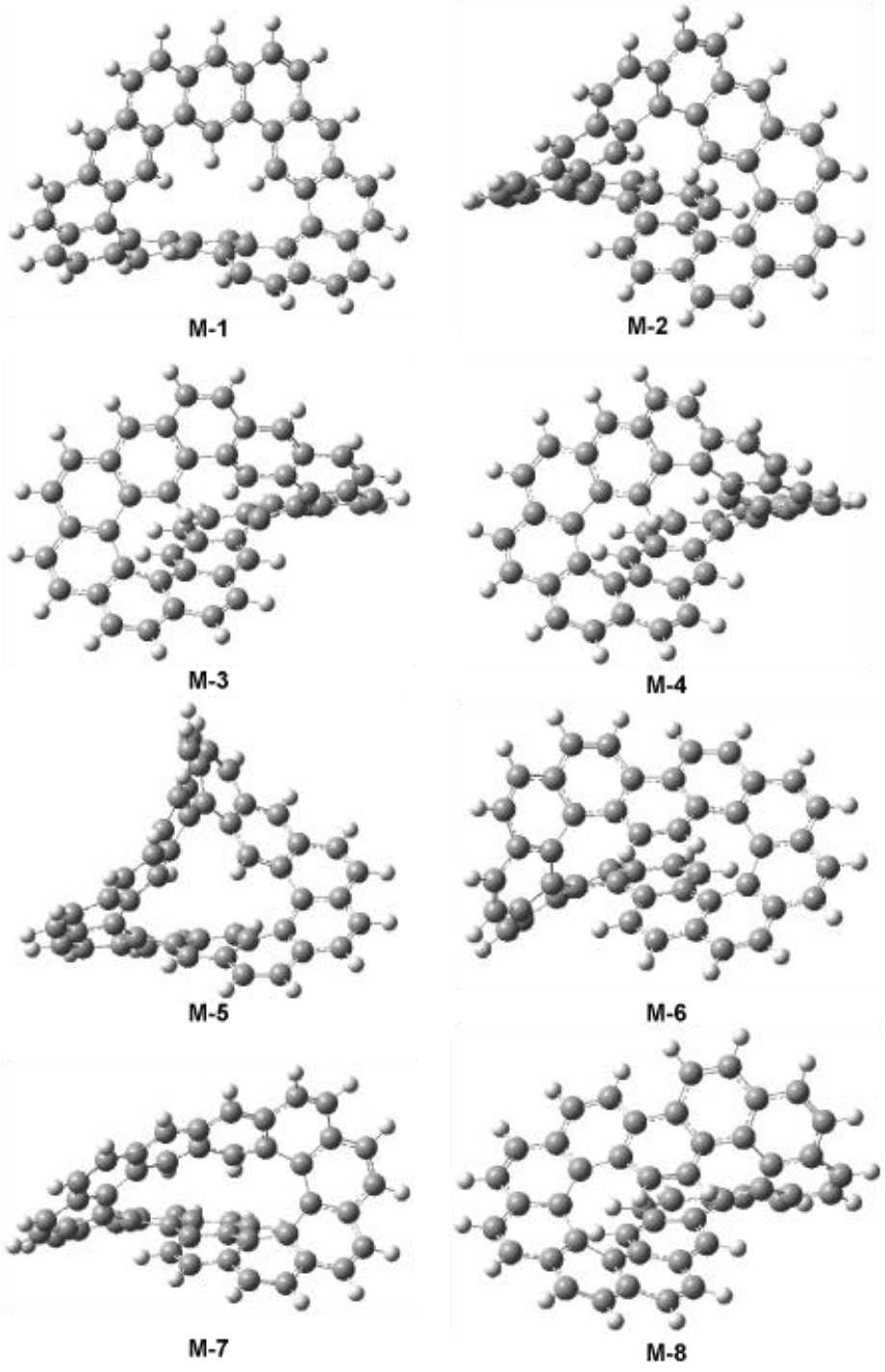

Figure 8. Structure of the eight lowest energy Möbius infinitene isomers

Table 6. Relative energy and strain energy (kcal mol^{-1}) of the Möbius [12]circulenes (**M-1** – **I-12**)

Cmpd	Designation	E_{rel}	SE
M-1	CCCACACACCCA	31.33	27.95
M-2	CCCCACCACCCC	33.02	42.34
M-3	CCCCACACCCCA	45.41	48.38
M-4	CCCCACCACCCA	47.32	50.29
M-5	CCCACCCACCCA	63.37	66.34
M-6	CCCCCDCCCCCC	66.08	88.11
M-7	CCCCCAACCCCC	75.48	84.80
M-8	CCCCCADDDDDC	79.11	94.78
M-9	CCCCAACCCCAA	80.21	76.83
M-10	CCCCCACCCCCC	81.53	97.21
M-11	CCACCACCACCA	82.61	79.23
M-12	CCCCCACCCCCA	97.32	106.65
M-13	CCCCCCDCCCCC	100.72	122.74
M-14	CAACAACAACAA	112.92	84.14
M-15	CCCCCCCCCCCA	138.61	154.29

The most compelling result pertaining to the Möbius infinitenes is that two of these structures, **M-1** and **M-2**, are lower in energy than **I-2**, the infinitene prepared by Itami.[11] In fact, **M-1** is lower in energy than **I-1** as well, though by less than 1 kcal mol^{-1}. The stability of these two Möbius infinitenes results from their low strain energy. In fact, **M-1** has the smallest strain energy of all of the infinitenes and Möbius infinitenes, and it is less strained than all but the five most stable ring analogues.

A component of the strain energy of a circulene is the energy required for distorting the geometry into some curved shape. For **M-1**, a number of schemes for assessing the distortion energy were examined. In each scheme, **M-1** is decomposed into fragments, and the energy difference for each fragment between its fully optimized geometry and its geometry in **M-1** was computed. The four different decomposition schemes are shown in the Supporting Materials (along with further details of how these computations were performed), and one example is displayed in Scheme 1. In Scheme 1**, M-1** is divided into two fragments, each of which optimize to planar structures. The top fragment has a

distortion energy of 22.8 kcal mol^{-1}, while the bottom fragment is more seriously deformed, having a distortion energy of 34.9 kcal mol^{-1}. The total distortion energy of **M-1** is thus estimated at 57.7 kcal mol^{-1}. The other three schemes predict a larger distortion energy, ranging from 59 to 74 kcal mol^{-1}. As a comparison, the total distortion energy of **I-2** can be estimated as twice the distortion energy of its [6]helicene fragment (Scheme 1); the computed value is 53.4 kcal mol^{-1}.

Scheme 1. Distortion energy computation of **M-1** and **I-2**

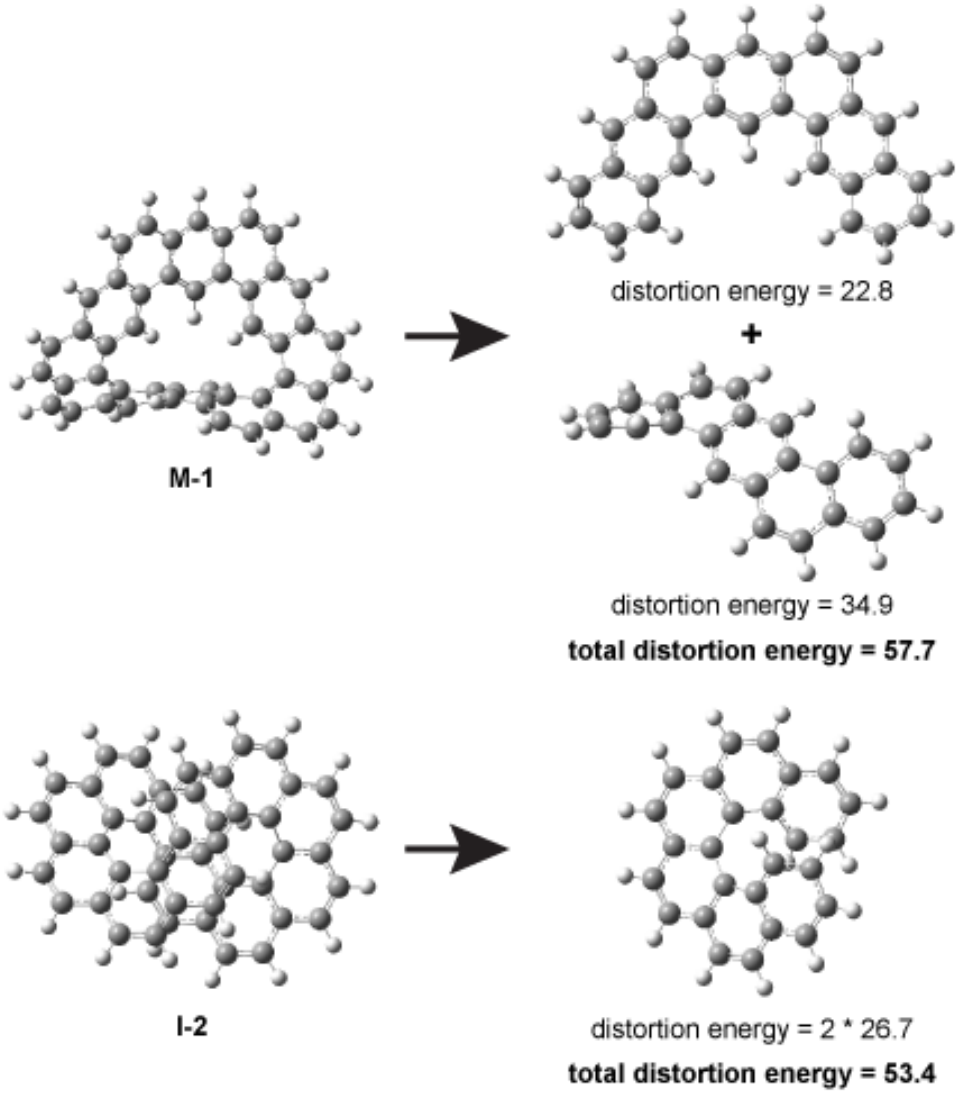

For **I-2**, this distortion energy is very similar to its strain energy, 53.4 vs. 55.1 kcal mol^{-1} (Table 1). On the other hand, the distortion energy of **M-1** is significantly larger than its strain energy, 57.7 vs. 28.0 kcal mol^{-1}. This result suggests that **M-1** possesses some stabilization. Though the structure of **M-1**

positions three hydrogen atoms in the interior that point towards the lower phenyl ring, a model of this interaction suggests that it is slightly destabilizing (see Supporting Materials). The possible stabilization from delocalization or aromaticity are addressed in the next section.

Another consideration is the difference in twisting of the infinitenes and Möbius infinitenes. Molecules such as the infinitenes have a shape defined by twist *Tw* and writhe *Wr*, the sum of which provides the linking number L_k.[12] Twist is rotation about the imaginary central axis lying within the plane of the phenyl rings. Writhe is rotation of the ribbon that creates crossings. Listed in Table 7 are the values of the twist and writhe for the six lowest energy infinitenes and Möbius infinitenes. There is no simple trend that relates twist or writhe to the overall stability or strain energy of these circulenes. However, since **M-1**, **M-2**, **I-1**, and **I-2** all lie within two kcal mol^{-1} of each other, the overall half twist or full twist is not affecting their stability.

Table 4. Values of twist (*Tw*), writhe (*Wr*) and linking numbers (*Lk*) of the three lowest energy ring, infinitene and Möbius infinitene isomers

cmpd	*Tw*	*Wr*	L_k
I-1	1.22	0.78	2
I-2	1.17	0.83	2
I-3	1.40	0.60	2
I-4	1.15	0.85	2
I-5	1.19	0.81	2
I-6	1.44	0.56	2
M-1	0.61	0.39	1
M-2	0.55	0.45	1
M-3	0.40	0.60	1
M-4	0.54	0.46	1
M-5	0.86	0.14	1
M-6	0.53	0.47	1

NMR, HOMA and aromaticity

NMR ^{1}H and ^{13}C chemical shifts were computed to help identify the structure of any [12]circulenes that might be prepared and to aid in assessing their aromatic character. The first step was to assess the performance of the computational methodology. Following guidance provided by Tantillo at the CHESHIRE web site,[24] chemical shifts were computed at B3LYP/6-31+G(d,p) with solvent (chloroform) modeled using SMD for comparison with the experimental values of **R-1**[7] and **I-2**.[11] Excellent linear correlations are seen for both the proton and carbon chemical shifts for **I-2** and for the proton shifts for **R-1** (see Supporting Materials). The slopes for these correlations are very close to one. The computed proton chemical shifts of **R-11**, 8.39 and 7.53 ppm, are in excellent agreement with experiment, 8.27 and 7.52 ppm. [4a] Thus, the computed chemical shifts of the [12]circulenes can be used without any further corrections.

The computed chemical shifts for all of the [12]circulenes are reported in the Supporting Materials. The chemical shifts for the three lowest energy ring, infinitene, and Möbius infinitene isomers are displayed in Figure 9. Some characteristic signal similarities are apparent for each set of isomers. For the low energy ring isomers, which have a pseudo-planar structure, the chemical shifts of the interior protons are far downfield, from 9.7 to 11.8 ppm. For the infinitenes, the chemical shifts of the protons in the crossing region of the figure-eight are shifted slightly upfield, between 6 and 7 ppm. The most distinctive proton signals for **M-1** and **M-2** arise from the protons positioned above the crossing and pointing down towards the face of the phenyl rings below; their signals are shifted downfield to 10.8 and 9.4 ppm in **M-1** and 9.2 ppm in **R-2**.

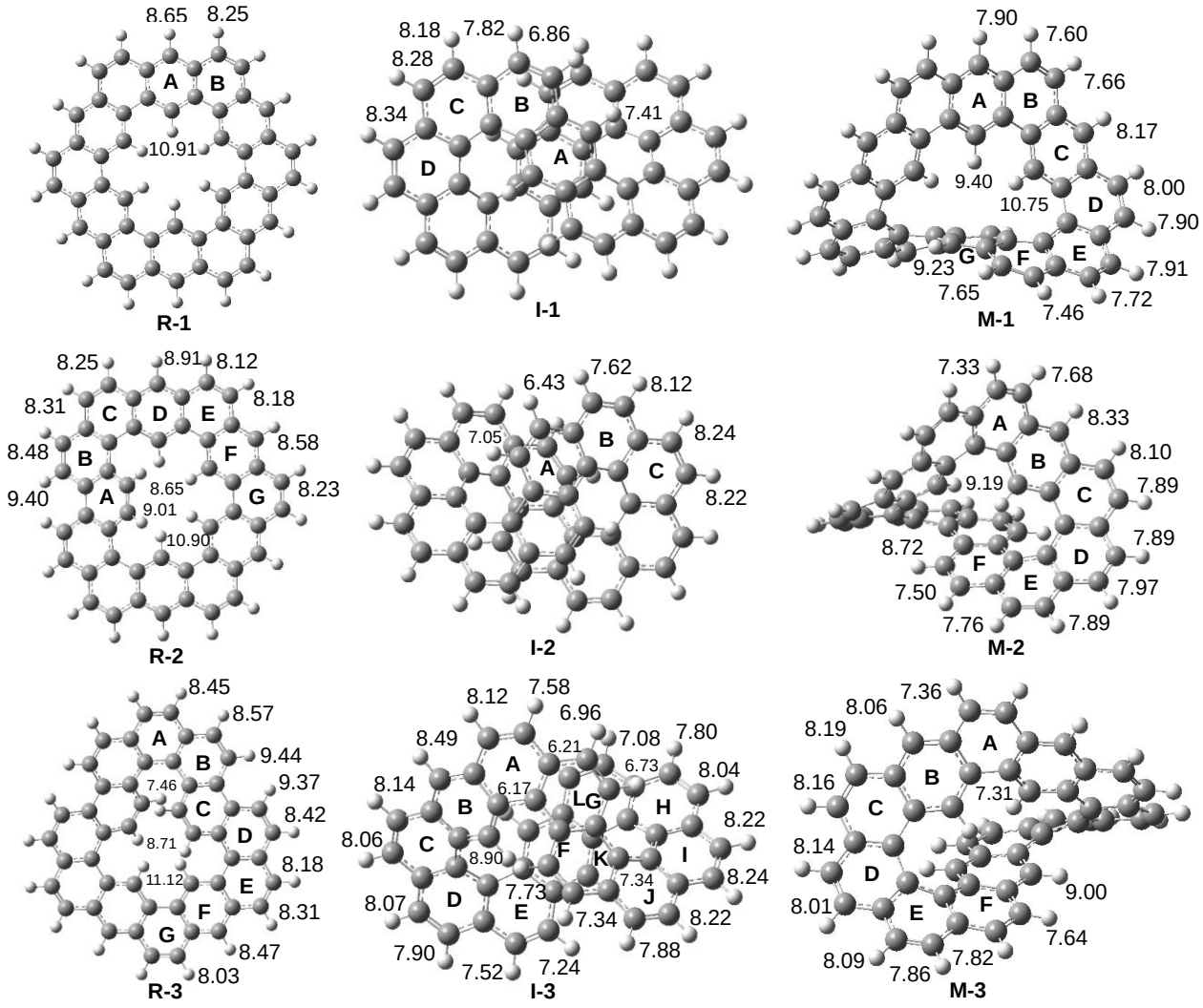

Figure 9. Computed ^{1}H chemical shifts (ppm) of select low-energy [12]circulenes

Chemical shifts are often indicative of aromatic character. Almost all of the [12]circulenes examined here exhibit chemical shifts in the typical aromatic region (7-9 ppm). There are two notable exceptions: the two highest energy isomers **R-18** and **R-19**. **R-19** is a cyclic acene with only A-type (*para* fusion) connectivity and **R-18** has 10 out of the 12 rings with A connectivity. This connectivity results in a ribbon-like structure necessitating significant non-planarity of the phenyl rings, which might imply a lessening of their aromatic character. In fact, the proton chemical shifts of **R-19** are at 2.7 ppm, while most of the chemical shifts of **R-18** are below 6 ppm, with two as low as 1.6 ppm. Despite the fact that

all of the examined isomers (except **R-1**) are non-planar and require some amount of distortion of the phenyl rings from planarity, only when that distortion becomes extreme do non-aromatic-like proton chemical shifts result.

Nucleus Independent Chemical Shifts (NICS) is a widely utilized method to assess aromaticity based on magnetic effects.[25] NICS values around -10 ppm are indicative of aromatic character, while values near zero indicate non-aromatic character. NICS is typically evaluated either at the center of the ring, NICS(0), or at a point 1 Å above or below the ring, NICS(1). NICS(1)[26] is often preferred as it minimizes the role of the σ-electrons. However, the geometries of the infinitenes and Möbius infinitenes often involve stacked rings or close approaches of atoms and a ring face, making NICS(1) problematic. Therefore, NICS(0) values were computed and reported in the Supporting Materials. NICS(0) values at the center of each phenyl ring for the three lowest energy isomers of the three classes are listed in Table 6.

Another commonly used method for assessing aromaticity is the Harmonic Oscillator Model of Aromaticity (HOMA), based on bond distances about the ring.[27] HOMA values range from 1, representing the aromatic character of benzene, to 0, having alternating bonds about the ring. The HOMA values for each phenyl ring of the three lowest energy isomers are also listed in Table 6.

Table 6. NICS and HOMA values of select low-energy [12]circulenes

ring	HOMA	NICS	HOMA	NICS	HOMA	NICS
	R-1		**R-2**		**R-3**	
A	0.36	-3.28	0.55	-5.09	0.66	-6.03
B	0.92	-9.21	0.76	-6.83	0.71	-6.68
C			0.49	-4.93	0.59	-5.45
D			0.90	-9.50	0.73	-5.90
E			0.35	-2.62	0.50	-5.34
F			0.92	-9.19	0.89	-9.68
G			0.39	-3.69	0.33	-1.55
	I-1		**I-2**		**I-3**	
A	0.87	-11.42	0.69	-7.01	0.54	-5.20
B	0.48	-5.53	0.64	-6.84	0.89	-9.76
C	0.66	-5.75	0.48	-4.93	0.52	-3.46
D	0.46	-5.75			0.70	-6.48
E					0.43	-3.56
F					0.90	-11.04
G					0.47	-4.39
H					0.78	-5.45
I					0.69	-4.55
J					0.72	-4.87
K					0.68	-5.10
L					0.68	-6.82
	M-1		**M-2**		**M-3**	
A	0.93	-9.50	0.48	-4.89	0.34	-0.62
B	0.38	-2.54	0.85	-9.80	0.86	-10.1
C	0.91	-9.66	0.36	-3.93	0.33	-5.39
D	0.44	-4.01	0.73	-5.51	0.50	-6.09
E	0.79	-5.83	0.69	-4.97	0.67	-6.02
F	0.26	-2.33	0.67	-5.48	0.52	-4.01
G	0.88	-8.53			0.87	-9.62

Inspection of the values of NICS and HOMA in Table 6 indicates a correlation between the two, though the linear fit is poor for the infinitenes and Möbius infinitenes. In general though, both measures agree on whether an individual phenyl ring has strong or weak aromatic character. For example, the phenyl rings of **R-1** alternate between having little aromatic character (NICS of -3.3ppm, HOMA of 0.4) or strong aromatic character (NICS of -9.2 ppm, HOMA of 0.9). This result is consistent with the recent

AFM study[8] that shows alternating aromatic and non-aromatic rings in **R-1**. Similar alternation of aromatic character is seen in all three Möbius infinitenes **M-1**, **M-2**, and **M-3** and in **I-3**. In contrast, **I-1** has every fourth ring with large aromaticity (NICS of -11.4 ppm) with the other rings showing modest aromaticity (NICS of -5.5 to -5.8 ppm). The rings of **I-2** show even less variation, with NICS values ranging from -5 to -7 ppm.

NICS, particularly when applied to polycyclic compounds, is a local index and may not reflect a more global assessment of a molecule's aromaticity.[28] Magnetically induced current density may provide a more global metric of such molecules. For example, kekulene **R-1** exhibits a diatropic current along the outer periphery and a paratropic current around the inner ring.[29] Computation[30] of the magnetically induced current density of **I-2** shows two non-intersecting diatropic current-density pathways, indicating aromatic character.

These data are not providing a consistent message regarding the aromatic character of the infinitenes. The root cause is the poor definition of aromaticity,[31] one that is just a collection of properties, including stabilization energy, structural properties like planarity and bond length, and magnetic properties including chemical shifts, NICS, and induced current density.

In examining this new class of twisted polycyclic aromatic compounds, our interest resides in their possible preparation. That centers our focus on their energetics and possible aromatic stabilization energy. Examination of acyclic linear and bent acenes provide some guidance here. Aromatic stabilization generally decreases with increasing size of the acene.[32] This can be seen in the decreasing stability of the linear acenes relative to anthracene (Table 7).

Table 7. Stabilization energy[a] (kcal mol^{-1}) of the linear acenes

Length	Stabilization energy
5	3.9
6	6.5
7	9.4
8	12.4
9	15.4
10	18.5
11	21.5
12	24.6

[a]Stabilization energy defined by reaction analogous to Reaction 3, see Supporting Materials for details.

Clar's sextet theory[33] argues that the dominant resonance structure of an aromatic compound is the one that maximizes the number of 6-member rings with 3 alternating double bonds. For the linear acenes, every resonance structure can have only one such "aromatic" 6-member ring (Figure 10). Therefore, fusing another ring adds two more double bonds that can aid to delocalize the π-electrons but does nothing to create additional aromaticity.

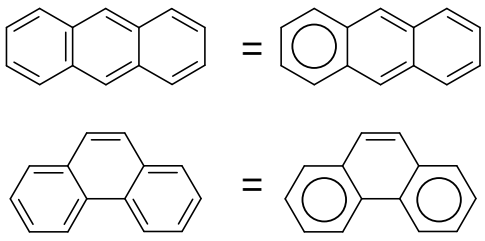

Figure 10. Dominant resonance structure and its Clar representation for anthracene and phenanthrene.

On the other hand, bent acenes, like phenanthrene, have a resonance structure with more than one Clar-type 6-member ring (see Figure 10). An interesting consequence of this is that acenes with multiple kinks, which allows for more Clar-type rings, are more stable than the reference compounds

anthracene and phenanthrene. This can be seen for isomers of nonacene (Table 8) and other examples are provided in the Supporting Materials. (Isomers with adjacent meta fusion were omitted to examine only planar structures.)

Table 8. Stabilization energy[a] (kcal mol^{-1}) and NICS (PPM) of some non-linear nonacenes.

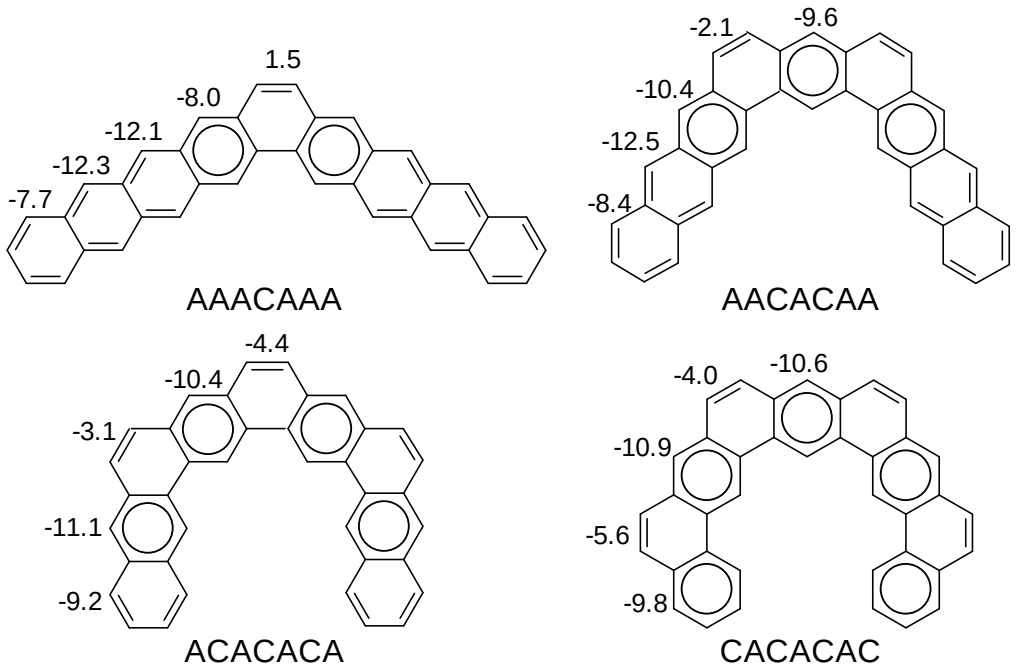

Nonacene	SE
AAACAAA	-0.1
AACACAA	-7.0
ACACACA	-9.1
CACACAC	-7.7

[a]Stabilization energy defined by reaction analogous to Reaction 3, see Supporting Materials for details and additional examples.

The NICS values of the bent nonacenes correspond to the Clar sextets. In particular, every ring that occupies a kink position has a decidedly reduced, i.e., less negative, NICS value, consistent with their diminished aromatic character.

Despite the indication from the NICS values, which might suggest reduced aromaticity of these bent nonacenes, they are all more stable than the reference compounds anthracene and phenanthrese. Since these two molecules are commonly considered to be aromatic, it is logical to conclude that the bent nonacenes, are likewise aromatic.

It is therefore consistent to conclude that kekulene **R-1** is also aromatic, as it too is more stable than the reference compounds (six anthracene and six phenanthrene molecules). Despite the fact that the NICS values of the phenyl rings alternate -9.2 and -3.3 ppm, suggesting that every other ring is strongly aromatic and weakly aromatic, the energetic criterion decidedly argues for the aromaticity of kekulene.

None of the other ring circulenes, nor any of infinitene or Möbius infinitenes, are more stable than their reference aromatic compounds. All of these molecules display NICS values at the kinked phenyl positions that are near zero, but that alone cannot discount the possibility of overall aromaticity. In fact, as discussed above, the kinked positions allow for adjacent rings to adopt the Clar sextet. So, all six of the anthracenyl phenyl rings of kekulene **R-1** adopt the Clar sextet, alternating with the phenanthrenyl phenyl rings that do not fulfil the sextet. Similarly, the phenyl rings in **I-1**, **I-2**, and **M-1** (among others) also have alternating rings that fulfil the Clar sextet. This too suggests that these molecules are aromatic.

The case for aromaticity of **M-1** is further buttressed by its energy partitioning. The overall strain energy of **M-1** is 28.0 kcal mol^{-1}. This strain can be portioned into a distortion energy and a stabilization energy. The distortion energy, as defined in Scheme 1, is 57.7 kcal mol^{-1}. That implies a stabilization energy of nearly 30 kcal mol^{-1}. That stabilization energy can be associated with delocalization and/or aromaticity. Taken together with the alternating Clar sextet and NICS value among the phenyl rings, the far downfield chemical shifts, it seems apparent that **M-1** is aromatic.

Highly twisted circulenes

With larger circulenes, ones with more phenyl rings, other topologies are possible. In particular, highly twisted geometries can be obtained. To highlight these topologies, the geometries of four highly twisted circulenes (HTC), see Figure 11, were computed. The intent here is to demonstrate the range of structural possibilities and not to identify the lowest energy possibilities.

HTC-1 is a [20]circulene and has *Lk* = 3. This is a Möbius topology with one and one-half twists. Its isomer **HTC-2** has *Lk* = 4, making two full twists. **HTC-2** is 111 kcal mol^{-1} lower in energy than **HTC-1**. **HTC-3** is a [28]circulene with *Lk* = 5, making two and one-half twists. Its isomer **HTC-4** has *Lk*=6, making three full twists. **HTC-4** lies 85 kcal mol^{-1} below **HTC-3**. The structures are displayed in Figure 12, though their three-dimensional shape is probably better viewed through a movie (see the Supporting Material) or with interactive molecular visualization software.

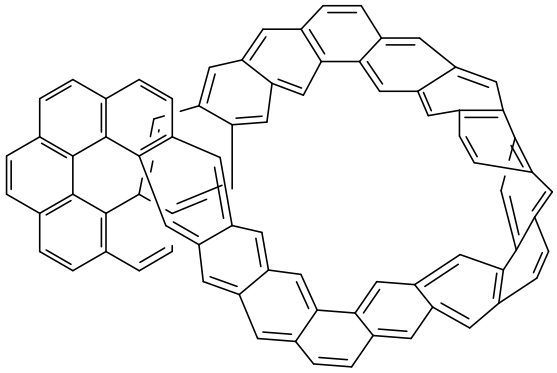

HTC-1 CCCCCAAADAACADAACAAA

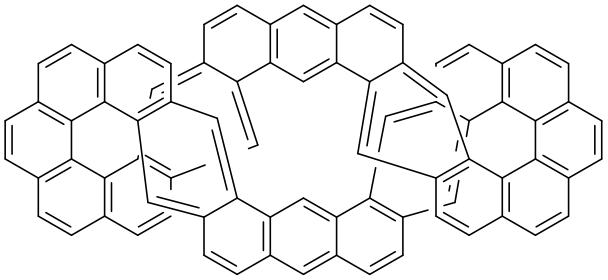

HTC-2 CCCCCADADACCCCCADADA

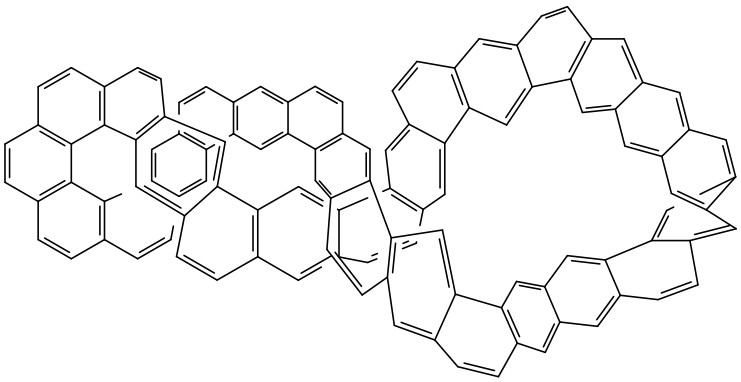

HTC-3 CCCCCADADACACAACADAADADACACA

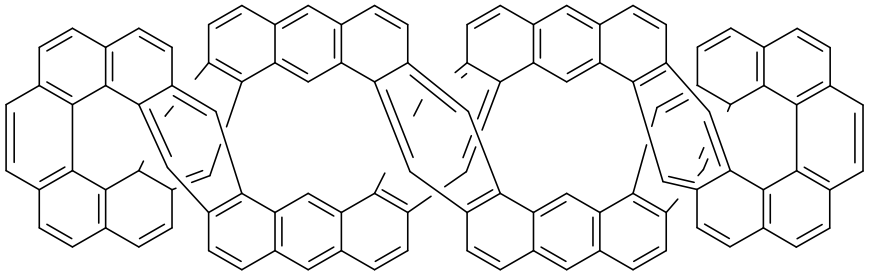

HTC-4 CCCCCADADACACADDDDDADADADADA

Figure 11. Examples of highly twisted circulenes (HTC)

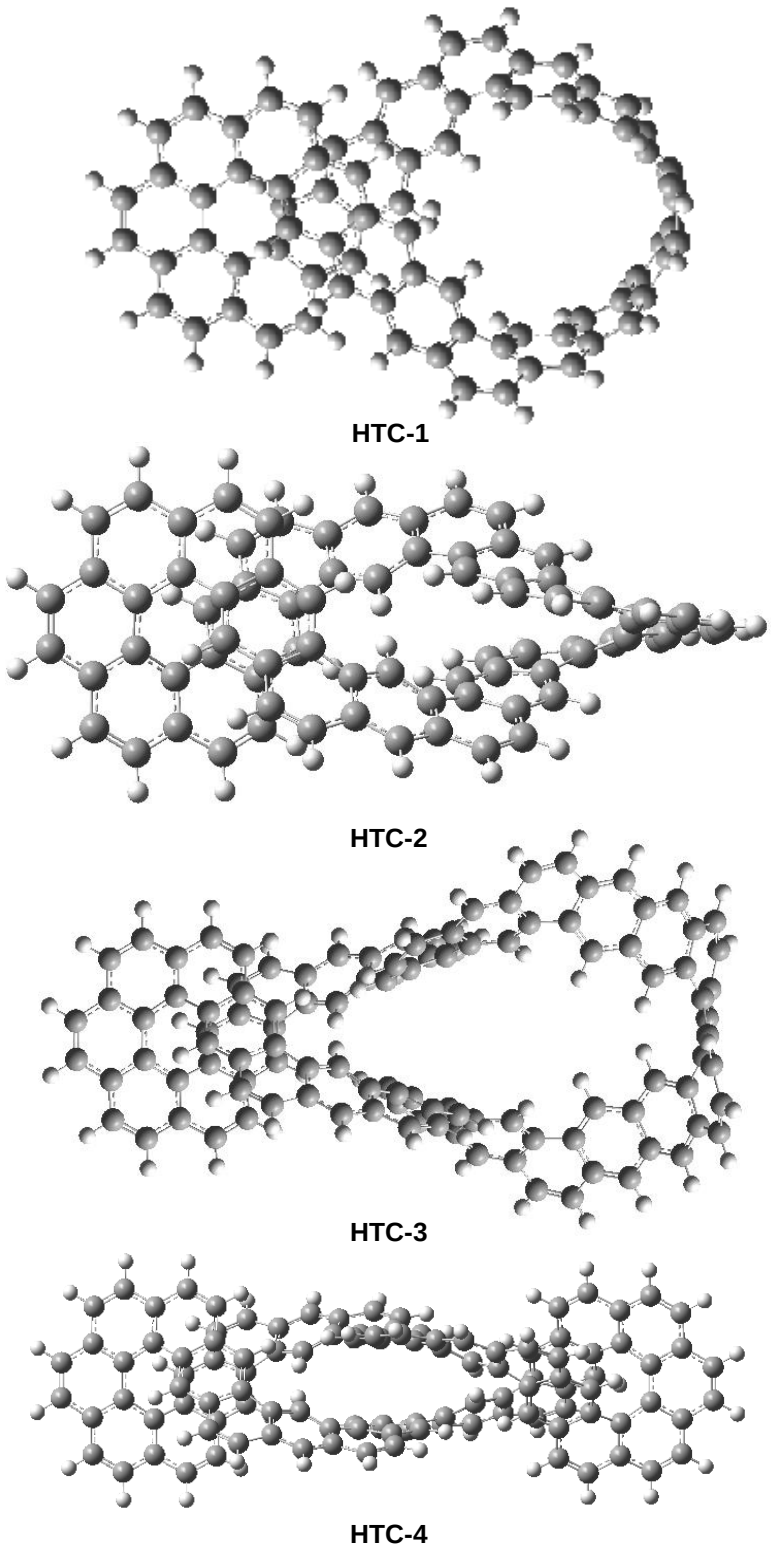

Figure 12. Structures of **HTC-1** – **HTC-4**

An interesting structural feature of these highly twisted circulenes are their π-stacking regions. **HTC-1** has one crossover where the phenyl rings stack. The centers of these two phenyl rings are separated by 3.25 Å, and the ring centers are offset very slightly. On the other hand, the two crossover regions in **HTC-2** position the phenyl rings significantly offset. This can be seen in the closeup truncated view of the crossover region of **HTC-2** in Figure 13. The center of each phenyl ring sits above a carbon atom of the phenyl ring in the other phenyl of the stacked pair, with a separation of 3.186 Å. This so-called parallel displaced arrangement of the benzene dimer is more energetically favorable than the arrangements where the two rings are directly above one another.[34] This parallel displaced arrangement is also seen in **HTC-3** and **HTC-4**, where the separation is 3.231 and 3.205 Å, respectively. The distance between the two phenyl rings in the central crossover of **HTC-4** is 3.536 Å, a long distance, suggesting little favorable stacking energy resulting from this crossover.

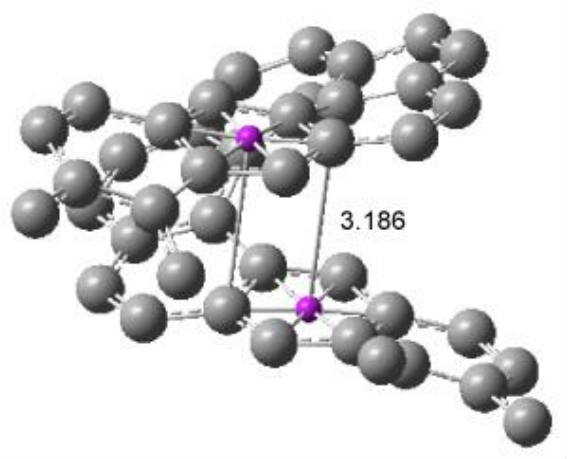

Figure 13. Crossover region of **HTC-2** showing one of the helicene regions. The rest of the molecule has been deleted and the hydrogens omitted. The purple ball defines the center of phenyl ring, and the labeled distance (Å) is the closest approach between the center of one phenyl ring and a carbon atom of the other phenyl of the stacked pair.

The computed strain energies of the two Möbius structures **HTC-1** and **HTC-3** are quite large, 133 and 85 kcal mol^{-1}, respectively. Further exploration of the possible isomers might identify more amenable targets examples. However, the strain energies of the two Hückel structures **HTC-2** and **HTC-4** reveal them to be viable synthetic targets. The strain energy of **HTC-4** is only 9 kcal mol^{-1}, and **HTC-2** is estimated to be more stable than its reference compounds by about 10 kcal mol^{-1}.

Conclusions

Fused polyphenyl systems can express a range of interesting topologies. [12]circulenes exhibiting a linking number of zero (ring[7] and ribbon[4a]) or two (infinitene[11] **I-2**) have been synthesized. The computations presented here identified eight isomers of **I-2** with *Lk* = 2, including one isomer **I-1** that is predicted to be energetically more stable than the original infinitene **I-2**. We have also identified fifteen [12]circulene isomers that have a Möbius topology, with *Lk* = 1. The most stable Möbius infinitene **M-1** is lower in energy than any of the infinitene isomers.

The aromatic character of the circulenes is a matter of debate, resting largely upon what criteria one chooses to utilize. The ^{1}H chemical shifts of almost all of the [12]circulenes examined here fall in the range typically associated with aromatic compounds (6-8ppm). The exception are the ribbon structures with a preponderance of *para* fusion, causing significant distortion of many of the phenyl rings away from planarity. NICS and HOMA values indicate an alternating strong aromaticity and weak aromaticity for the phenyl rings in many of the low energy ring structures, infinitenes, and Möbius infinitenes. However, this behavior reflects a maximization of Clar structures. Lastly, comparison of the energies of the [12]circulenes with reference compounds (phenanthrene and anthracene) along with estimation of distortion energies suggests that many of the [12]circulenes exhibit stabilization energies comparable to those of linear or bent acenes. It appears that these compounds deserve to be categorized as aromatic.

These computations suggest that a number of infinitenes and Möbius infinitenes should be viable synthetic targets. Additionally, the low strain energies of more highly twisted circulene suggest that they too may be good candidates for synthesis. The circulenes appear to be ground for fruitful exploration, elaborating molecules with unusual topologies that may lead to interesting properties and utilities.

Supporting Information

Part 1: Complete citation for Ref. 15, InChIs and InChIKeys of the [12]circulenes, Tables S1-S6, Figures S1-S5. Part 2: Coordinates of the [12]circulenes and **HTC1-4**, computed ^{1}H and ^{13}C NMR chemical shifts and NICS(0) values of the [12]circulenes. Movies depicting rotation of **HTC-1** – **HTC-4**.

Notes

The author declares no competing financial interest.

Acknowledgments

The author thanks Monmouth University for the resources where the computations were performed.

References

(1) Majewski, M. A.; Stępień, M. Bowls, Hoops, and Saddles: Synthetic Approaches to Curved Aromatic Molecules. *Angew. Chem. Int. Ed.* **2019**, *58*, 86-116.

(2) (a) Allen, M. J.; Tung, V. C.; Kaner, R. B. Honeycomb Carbon: A Review of Graphene. *Chem. Rev.* **2010**, *110*, 132-145. (b) Ghuge, D. A.; Shirode, R. A.; Kadam, J. V. Graphene: A Comprehensive Review. *Curr. Drug Targets* **2017**, *18*, 724-733. (c) Madurani, K. A.; Suprapto, S.; Machrita, N. I.; Bahar, S. L.; Illiya, W.;

Kurniawan, F. Progress in Graphene Synthesis and its Application: History, Challenge and the Future Outlook for Research and Industry. *ECS J. Solid State Sci. Tech.* **2020**, *9*, 093013.

(3) (a) Wu, Y.-T.; Siegel, J. S. Aromatic Molecular-Bowl Hydrocarbons: Synthetic Derivatives, Their Structures, and Physical Properties. *Chem. Rev.* **2006**, *106*, 4843-4867. (b) Wu, Y.-T.; Siegel, J. S. Synthesis, Structures, and Physical Properties of Aromatic Molecular-Bowl Hydrocarbons. *Top. Curr. Chem.* **2014**, *349*, 63-120. (c) Stuparu, M. C. Corannulene: A Curved Polyarene Building Block for the Construction of Functional Materials. *Acc. Chem. Res.* **2021**, *54*, 2858-2870.

(4) (a) Povie, G.; Segawa, Y.; Nishihara, T.; Miyauchi, Y.; Itami, K. Synthesis of a carbon nanobelt. *Science* **2017**, *356*, 172-175. (b) Cheung, K. Y.; Gui, S.; Deng, C.; Liang, H.; Xia, Z.; Liu, Z.; Chi, L.; Miao, Q. Synthesis of Armchair and Chiral Carbon Nanobelts. *Chem* **2019**, *5*, 838-847.

(5) (a) Yamago, S.; Kayahara, E.; Iwamoto, T. Organoplatinum-Mediated Synthesis of Cyclic π-Conjugated Molecules: Towards a New Era of Three-Dimensional Aromatic Compounds. *Chem. Rec.* **2014**, *14*, 84-100. (b) Takaba, H.; Omachi, H.; Yamamoto, Y.; Bouffard, J.; Itami, K. Selective Synthesis of [12]Cycloparaphenylene. *Angew. Chem. Int. Ed.* **2009**, *48*, 6112-6116. (c) Golder, M. R.; Jasti, R. Syntheses of the Smallest Carbon Nanohoops and the Emergence of Unique Physical Phenomena. *Acc. Chem. Res.* **2015**, *48*, 557-566. (d) Lewis, S. E. Cycloparaphenylenes and related nanohoops. *Chem. Soc. Rev.* **2015**, *44*, 2221-2304. (e) Hermann, M.; Wassy, D.; Esser, B. Conjugated Nanohoops Incorporating Donor, Acceptor, Hetero- or Polycyclic Aromatics. *Angew. Chem. Int. Ed.* **2021**, *60*, 15743-15766.

(6) Kumar, R.; Aggarwal, H.; Srivastava, A. Of Twists and Curves: Electronics, Photophysics, and Upcoming Applications of Non-Planar Conjugated Organic Molecules. *Chem. Eur. J.* **2020**, *26*, 10653-10675.

(7) Diederich, F.; Staab, H. A. Benzenoid versus Annulenoid Aromaticity: Synthesis and Properties of Kekulene. *Angew. Chem. Int. Ed. Engl.* **1978**, *17*, 372-374.

(8) Pozo, I.; Majzik, Z.; Pavliček, N.; Melle-Franco, M.; Guitián, E.; Peña, D.; Gross, L.; Pérez, D. Revisiting Kekulene: Synthesis and Single-Molecule Imaging. *J. Am. Chem. Soc.* **2019**, *141*, 15488-15493.

(9) Christoph, H.; Grunenberg, J.; Hopf, H.; Dix, I.; Jones, P. G.; Scholtissek, M.; Maier, G. MP2 and DFT calculations on circulenes and an attempt to prepare the second lowest benzolog, [4]circulene. *Chem. - Eur. J.* **2008**, *14*, 5604-5616.

(10) Heilbronner, E. Molecular Orbitals in homologen Reihen mehrkerniger aromatischer Kohlenwasserstoffe: I. Die Eigenwerte yon LCAO-MO's in homologen Reihen. *Helv. Chim. Acta* **1954**, *37*, 921-935.

(11) Krzeszewski, M.; Ito, H.; Itami, K. Infinitene: A Helically Twisted Figure-Eight [12]Circulene Topoisomer. *J. Am. Chem. Soc.* **2022**, *144*, 862-871.

(12) Rappaport, S. M.; Rzepa, H. S. Intrinsically Chiral Aromaticity. Rules Incorporating Linking Number, Twist, and Writhe for Higher-Twist Möbius Annulenes. *J. Am. Chem. Soc.* **2008**, *130*, 7613-7619.

(13) (a) Walba, D. M.; Richards, R. M.; Haltiwanger, R. C. Total synthesis of the first molecular Moebius strip. *J. Am. Chem. Soc.* **1982**, *104*, 3219-3221. (b) Walba, D. M.; Homan, T. C.; Richards, R. M.; Haltiwanger, R. C. Topological Stereochemistry. 9. Synthesis and Cutting in Half of a Molecular Mobius Strip. *New J. Chem.* **1993**, *17*, 661-681. (c) Martin-Santamaria, S.; Lavan, B.; Rzepa, H. S. Mobius Aromatics Arising from a C=C=C Ring Component. *Chem. Commun.* **2000**, 1089-1090. (d) Ajami, D.; Oeckler, O.; Simon, A.; Herges, R. Synthesis of a Möbius aromatic hydrocarbon. *Nature* **2003**, *426*, 819-821. (e) Rzepa, H. S. A Double-Twist Möbius-Aromatic Conformation of [14]Annulene. *Org. Lett.* **2005**, *7*, 4637-4639. (f) Castro, C.; Chen, Z.; Wannere, C. S.; Jiao, H.; Karney, W. L.; Mauksch, M.; Puchta, R.; Hommes, N. J. R. v. E.; Schleyer, P. v. R. Investigation of a Putative Möbius Aromatic Hydrocarbon. The Effect of Benzannelation on Möbius [4n]Annulene Aromaticity. *J. Am. Chem. Soc.* **2005**, *127*, 2425-2432. (g) Castro, C.; Karney, W. L.; Valencia, M. A.; Vu, C. M. H.; Pemberton, R. P. Möbius Aromaticity in [12]Annulene: Cis-Trans Isomerization via Twist-Coupled Bond Shifting. *J. Am. Chem. Soc.* **2005**, *127*,

9704-9705. (h) Castro, C.; Karney, W. L.; Vu, C. M. H.; Burkhardt, S. E.; Valencia, M. A. Computational Evaluation of the Evidence for Tri-trans-[12]Annulene. *J. Org. Chem.* **2005**, *70*, 3602-3609. (i) Ajami, D.; Hess, K.; Köhler, F.; Näther, C.; Oeckler, O.; Simon, A.; Yamamoto, C.; Okamoto, Y.; Herges, R. Synthesis and Properties of the First Möbius Annulenes. *Chem. Eur. J.* **2006**, *12*, 5434-5445. (j) Herges, R. Topology in Chemistry: Designing Möbius Molecules. *Chem. Rev.* **2006**, *106*, 4820-4842. (k) Tahara, K.; Tobe, Y. Molecular Loops and Belts. *Chem. Rev.* **2006**, *106*, 5274-5290. (l) Allan, C. S. M.; Rzepa, H. S. Chiral Aromaticities. A Topological Exploration of Möbius Homoaromaticity. *J. Chem. Theory Comput.* **2008**, *4*, 1841-1848. (m) Rzepa, H. S. Lemniscular Hexaphyrins as Examples of Aromatic and Antiaromatic Double-Twist Möbius Molecules. *Org. Lett.* **2008**, *10*, 949–952. (n) Stępień, M.; Sprutta, N.; Latos-Grażyński, L. Figure Eights, Möbius Bands, and More: Conformation and Aromaticity of Porphyrinoids. *Angew. Chem. Int. Ed.* **2011**, *50*, 4288-4340. (o) Schaller, G. R.; Herges, R. Moebius molecules with twists and writhes. *Chem. Commun.* **2013**, *49*, 1254-1260. (p) Schaller, G. R.; Topić, F.; Rissanen, K.; Okamoto, Y.; Shen, J.; Herges, R. Design and synthesis of the first triply twisted Möbius annulene. *Nature Chem.* **2014**, *6*, 608-613. (q) Tanaka, T.; Osuka, A. Chemistry of meso-Aryl-Substituted Expanded Porphyrins: Aromaticity and Molecular Twist. *Chem. Rev.* **2017**, *117*, 2584-2640. (r) Fan, Y.-Y.; Chen, D.; Huang, Z.-A.; Zhu, J.; Tung, C.-H.; Wu, L.-Z.; Cong, H. An isolable catenane consisting of two Möbius conjugated nanohoops. *Nature Commun.* **2018**, *9*, 3037. (s) Naulet, G.; Sturm, L.; Robert, A.; Dechambenoit, P.; Röhricht, F.; Herges, R.; Bock, H.; Durola, F. Cyclic tris-[5]helicenes with single and triple twisted Möbius topologies and Möbius aromaticity. *Chem. Sci.* **2018**, *9*, 8930-8936. (t) Nishigaki, S.; Shibata, Y.; Nakajima, A.; Okajima, H.; Masumoto, Y.; Osawa, T.; Muranaka, A.; Sugiyama, H.; Horikawa, A.; Uekusa, H.; Koshino, H.; Uchiyama, M.; Sakamoto, A.; Tanaka, K. Synthesis of Belt- and Möbius-Shaped Cycloparaphenylenes by Rhodium-Catalyzed Alkyne Cyclotrimerization. *J. Am. Chem. Soc.* **2019**, *141*, 14955-14960. (u) Dash, S.; Ghosh, A.; Srinivasan, A.; Suresh, C. H.; Chandrashekar, T. K. Protonation-Triggered Hückel and Möbius Aromatic Transformations in Nonaromatic Core-Modified [30]Hexaphyrin(2.1.1.2.1.1) and Annulated

[28]Hexaphyrin(2.1.1.0.1.1). *Org. Lett.* **2019**, *21*, 9637-9641. (v) Senthilkumar, K.; Kondratowicz, M.; Lis, T.; Chmielewski, P. J.; Cybińska, J.; Zafra, J. L.; Casado, J.; Vives, T.; Crassous, J.; Favereau, L.; Stępień, M. Lemniscular [16]Cycloparaphenylene: A Radially Conjugated Figure-Eight Aromatic Molecule. *J. Am. Chem. Soc.* **2019**, *141*, 7421-7427. (w) Jiang, X.; Laffoon, S. D.; Chen, D.; Pérez-Estrada, S.; Danis, A. S.; Rodríguez-López, J.; Garcia-Garibay, M. A.; Zhu, J.; Moore, J. S. Kinetic Control in the Synthesis of a Möbius Tris((ethynyl)[5]helicene) Macrocycle Using Alkyne Metathesis. *J. Am. Chem. Soc.* **2020**, *142*, 6493-6498. (x) Schaub, T. A.; Prantl, E. A.; Kohn, J.; Bursch, M.; Marshall, C. R.; Leonhardt, E. J.; Lovell, T. C.; Zakharov, L. N.; Brozek, C. K.; Waldvogel, S. R.; Grimme, S.; Jasti, R. Exploration of the Solid-State Sorption Properties of Shape-Persistent Macrocyclic Nanocarbons as Bulk Materials and Small Aggregates. *J. Am. Chem. Soc.* **2020**, *142*, 8763-8775. (y) Bachrach, S. M.; Rzepa, H. S. Cycloparaphenylene Möbius trefoils. *Chem. Commun.* **2020**, *56*, 13567-13570.

(14) Chai, J.-D.; Head-Gordon, M. Long-range corrected hybrid density functionals with damped atom-atom dispersion corrections. *Phys. Chem. Chem. Phys.* **2008**, *10*, 6615-6620.

(15) Frisch, M. J.; et al. *Gaussian-16, rev. B.01*; Gaussian, Inc.: Wallingford CT, 2016.

(16) Rzepa, H. S.; Rappaport, S. *LinkTW and LinkTWM Programs for computing Linking numbers, Twist and Writhe for cyclic annulenes.* 2014. https://figshare.com/articles/dataset/LinkTW_and_LinkTWM_Programs_for_computing_Linking_numbers_Twist_and_Writhe_for_cyclic_annulenes_/1207997 (accessed 12/1/2022).

(17) OEIS Foundation. Number of n-bead necklaces with 3 colors. In *The On-line Encyclopedia of Integer Sequences*; 2022; https://oeis.org/A001867.

(18) Heller, S. R.; McNaught, A.; Pletnev, I.; Stein, S.; Tchekhovskoi, D. InChI, the IUPAC International Chemical Identifier. *J. Cheminformatics* **2015**, *7*, 23.

(19) Bachrach, S. M. On the Resonance Energy of Methylenecyclopropene and Cyclopropenone. *J. Org. Chem.* **1990**, *55*, 4961-4963.

(20) Bachrach, S. M. The Group Equivalent Reaction: An Improved Method for Determining Ring Strain Energy. *J. Chem. Ed.* **1990**, *67*, 907-908.

(21) Wheeler, S. E.; Houk, K. N.; Schleyer, P. v. R.; Allen, W. D. A Hierarchy of Homodesmotic Reactions for Thermochemistry. *J. Am. Chem. Soc.* **2009**, *131*, 2547-2560.

(22) (a) Cioslowski, J.; O'Connor, P. B.; Fleischmann, E. D. Is Superbenzene Superaromatic? *J. Am. Chem. Soc.* **1991**, *113*, 1086-1089. (b) Aihara, J. Is superaromaticity a fact or an artifact? The kekulene problem. *J. Am. Chem. Soc.* **1992**, *114*, 865-868. (c) Jiao, H.; Schleyer, P. v. R. Is Kekulene Really Superaromatic? *Angew. Chem. Int. Ed.* **1996**, *35*, 2383-2386. (d) Zhou, Z. Are kekulene, coronene, and corannulene tetraanion superaromatic? Theoretical examination using hardness indices. *J. Phys. Org. Chem.* **1995**, *8*, 103-107. (e) Haags, A.; Reichmann, A.; Fan, Q.; Egger, L.; Kirschner, H.; Naumann, T.; Werner, S.; Vollgraff, T.; Sundermeyer, J.; Eschmann, L.; Yang, X.; Brandstetter, D.; Bocquet, F. C.; Koller, G.; Gottwald, A.; Richter, M.; Ramsey, M. G.; Rohlfing, M.; Puschnig, P.; Gottfried, J. M.; Soubatch, S.; Tautz, F. S. Kekulene: On-Surface Synthesis, Orbital Structure, and Aromatic Stabilization. *ACS Nano* **2020**, *14*, 15766-15775. (f) Fan, W.; Han, Y.; Wang, X.; Hou, X.; Wu, J. Expanded Kekulenes. *J. Am. Chem. Soc.* **2021**, *143*, 13908-13916. (g) Aihara, J.-i.; Makino, M.; Ishida, T.; Dias, J. R. Analytical Study of Superaromaticity in Cycloarenes and Related Coronoid Hydrocarbons. *J. Phys. Chem. A* **2013**, *117*, 4688-4697.

(23) Ehrlich, S.; Bettinger, H. F.; Grimme, S. Dispersion-Driven Conformational Isomerism in σ-Bonded Dimers of Larger Acenes. *Angew. Chem. Int. Ed.* **2013**, *41*, 10892–10895.

(24) Lodewyk, M. W.; Siebert, M. R.; Tantillo, D. J. *Chemical Shift Repository (Cheshire)*. 2019. http://cheshirenmr.info/ (accessed 12/1/2022).

(25) Schleyer, P. v. R.; Maerker, C.; Dransfeld, A.; Jiao, H.; Hommes, N. J. R. v. E. Nucleus-Independent Chemical Shifts: A Simple and Efficient Aromaticity Probe. *J. Am. Chem. Soc.* **1996**, *118*, 6317-6318.

(26) Schleyer, P. v. R.; Jiao, H.; van Eikema Hommes, N. J. R.; Malkin, V. G.; Malkina, O. L. An Evaluation of the Aromaticity of Inorganic Rings: Refined Evidence from Magnetic Properties. *J. Am. Chem. Soc.* **1997**, *119*, 12669-12670.

(27) (a) Kruszewski, J.; Krygowski, T. M. Definition of aromaticity basing on the harmonic oscillator model. *Tetrahedron Letters* **1972**, *13*, 3839-3842. (b) Krygowski, T. M.; Szatylowicz, H.; Stasyuk, O. A.; Dominikowska, J.; Palusiak, M. Aromaticity from the Viewpoint of Molecular Geometry: Application to Planar Systems. *Chem. Rev.* **2014**, *114*, 6383-6422, lode. (c) Dobrowolski, J. C. Three Queries about the HOMA Index. *ACS Omega* **2019**, *4*, 18699-18710.

(28) (a) Orozco-Ic, M.; Barroso, J.; Charistos, N. D.; Muñoz-Castro, A.; Merino, G. Consequences of Curvature on Induced Magnetic Field: The Case of Helicenes. *Chem. - Eur. J.* **2020**, *26*, 326-330. (b) Monaco, G.; Zanasi, R. Analysis of the Nucleus-Independent Chemical Shifts of [10]Cyclophenacene: Is It an Aromatic or Antiaromatic Molecule? *J. Phys. Chem. Lett.* **2017**, *8*, 4673-4678.

(29) (a) Steiner, E.; Fowler, P. W.; Jenneskens, L. W.; Acocella, A. Visualisation of counter-rotating ring currents in kekulene. *Chem. Commun.* **2001**, 659-660. (b) Orozco-Ic, M.; Dimitrova, M.; Barroso, J.; Sundholm, D.; Merino, G. Magnetically Induced Ring-Current Strengths of Planar and Nonplanar Molecules: New Insights from the Pseudo-π Model. *J. Phys. Chem A* **2021**, *125*, 5753-5764.

(30) (a) Orozco-Ic, M.; Valiev, R. R.; Sundholm, D. Non-intersecting ring currents in [12]infinitene. *Phys. Chem. Chem. Phys.* **2022**, *24*, 6404-6409. (b) Monaco, G.; Zanasi, R.; Summa, F. F. Magnetic Characterization of the Infinitene Molecule. *J. Phys. Chem A* **2022**, *126*, 3717-3723.

(31) Bachrach, S. M. *Computational Organic Chemistry*; Wiley, 2014.

(32) (a) Solà, M. Forty years of Clar's aromatic π-sextet rule. *Frontiers Chem.* **2013**, *1*, 1-8, Review. (b) Sakai, S.; Kita, Y. Structure prediction and aromaticity of acenes and phenylenes series. A combination method between asymmetric Kekulé structures. *J. Phys. Org. Chem.* **2012**, *25*, 840-849.

(33) Clar, E. *The Aromatic Sextet*; J. Wiley, 1972.

(34) (a) Karton, A.; Martin, J. M. L. Prototypical π–π dimers re-examined by means of high-level CCSDT(Q) composite ab initio methods. *J. Chem. Phys.* **2021**, *154*, 124117. (b) Sinnokrot, M. O.; Sherrill, C. D. Highly Accurate Coupled Cluster Potential Energy Curves for the Benzene Dimer: Sandwich, T-Shaped, and Parallel-Displaced Configurations. *J. Phys. Chem. A* **2004**, *108*, 10200-10207.